A

DISSERTATION REPORT

ON

LITHIUM NIOBATE BASED ALL OPTICAL DEVICES FOR PHOTONICS INTEGRATED CIRCUITS

IS SUBMITTED AS A PARTIAL FULFILMENT OF

MASTER OF TECHNOLOGY IN WIRELESS AND OPTICAL COMMUNICATION

BY

HARSH KUMAR

(2015PWC5305)

UNDER THE GUIDANCE OF

DR. GHANSHYAM SINGH

IN

DEPARTMENT OF ELECTRONICS AND COMMUNICATION ENGINEERING

DEPARTMENT OF ELECTRONICS AND COMMUNICATION ENGINEERING

MALAVIYA NATIONAL INSTITUTE OF TECHNOLOGY JAIPUR

JUNE 2017

A

DISSERTATION REPORT

ON

LITHIUM NIOBATE BASED ALL OPTICAL DEVICES FOR PHOTONICS INTEGRATED CIRCUITS

IS SUBMITTED AS A PARTIAL FULFILMENT OF

MASTER OF TECHNOLOGY IN WIRELESS AND OPTICAL COMMUNICATION

BY

HARSH KUMAR

(2015PWC5305)

UNDER THE GUIDANCE OF

DR. GHANSHYAM SINGH

IN

DEPARTMENT OF ELECTRONICS AND COMMUNICATION ENGINEERING

DEPARTMENT OF ELECTRONICS AND COMMUNICATION ENGINEERING

MALAVIYA NATIONAL INSTITUTE OF TECHNOLOGY JAIPUR

JUNE 2017

DEPARTMENT OF ELECTRONICS AND COMMUNICATION ENGINEERING

MALAVIYA NATIONAL INSTITUTE OF TECHNOLOGY

JAIPUR (RAJASTHAN)-302017

CERTIFICATE

This is to certify that the dissertation report entitled **"LITHIUM NIOBATE BASED ALL OPTICAL DEVICES FOR PHOTONICS INTEGRATED CIRCUITS"** prepared by **HARSH KUMAR** (2015PWC5305), submitted in the partial fulfilment of the Degree of **Master of Technology** in **Wireless and Optical Communication** at the **Department of Electronics and Communication Engineering** of **Malaviya National Institute Of Technology Jaipur** is a record of bonafide research work carried out by him under my supervision and is hereby approved for submission. The contents of this dissertation work, in full or in parts, have not been submitted to any other Institute or University for the award of any degree or diploma.

Date:

Place:

Dr. Ghanshyam Singh
Associate Professor
Department of ECE
MNIT Jaipur

DEPARTMENT OF ELECTRONICS AND COMMUNICATION ENGINEERING

MALAVIYA NATIONAL INSTITUTE OF TECHNOLOGY

JAIPUR (RAJASTHAN)-302017

DECLARATION

I **HARSH KUMAR** hereby declare that the dissertation entitled **"LITHIUM NIOBATE BASED ALL OPTICAL DEVICES FOR PHOTONICS INTEGRATED CIRCUITS"** being submitted by me in partial fulfilment of the degree of **Master of Technology** in **Wireless and Optical Communication** at the **Department of Electronics and Communication Engineering** of **Malaviya National Institute of Technology Jaipur** is a research work carried out by me under the supervision of **Dr. Ghanshyam Singh,** and contents of this dissertation work, in full or in parts, have not been submitted to any other Institute or University for the award of any degree or diploma. I also certify that no part of this dissertation work has been copied or borrowed from anywhere else. In case any type of plagiarism is found out, I will be solely and completely responsible for it.

Date:

Place:

HARSH KUMAR

M. Tech

Wireless and Optical Communication

2015PWC5305

Acknowledgement

I take this opportunity to express my deep sense of gratitude to my supervisor Dr. Ghanshyam Singh, Associate Professor, Department of Electronics and Communication Engineering, MNIT Jaipur, without his guidance this work would not have been successful. He continuously motivated me, provided timely feedback and also encouraged me to present my work at highly valued international conferences and peer reviewed journals.

I would also like to thank Dr. Buryy Oleh, Associate Professor, Department of Semiconductor Electronics, Institute of Telecommunication Radioelectronic & Electronic Engg, Lviv Polytechnic National University, Lviv (Ukraine) for providing all the technical expertise required for the completion of this work. I am grateful to India–Ukraine inter-governmental science & technology cooperation programme between the MNIT Jaipur (India) and the Lviv National Polytechnique Institute, Lviv (Ukraine): Project sanction no: INT/RUS/UKR/P-15/2015.

I would like to thank Dr. K.K. Sharma, Head of Department, Department of Electronics and Communication Engineering, MNIT Jaipur for providing all the resources necessary to carry out this work.

I would like to thank Mr. Sourabh Sahu, Research Scholar, Department of Electronics and Communication Engineering, MNIT Jaipur and my senior Mr. Abhishek Godbole (M. Tech Student 2014-2016) for numerous fruitful discussions on this topic. They were always ready to help and shared their knowledge on this topic whenever required.

I thank all my colleagues and the technical and non-technical staff of Department of Electronics and Communication Engineering, MNIT Jaipur for supporting and encouraging me throughout this work. Finally, I am grateful to my parents for believing in me and constantly encouraging me to give my best for the completion of this work.

Abstract

Light as a method of communication has been used since ancient times. Smoke and fire signals, light houses, etc. are used as the means optical communication to pass their messages. As technology developed, new inventions were made in the field of optics and photonics. Today a large portion of the fields which are identified with innovation utilize optics and photonics in somehow. Research in the field of optical communication has developed at a fast pace. In recent years analysts have planned and built up a few sorts of optical fibers; thin strands of glass that can be used for high data rate transmission. As the technology developed the performance of optical fibers improved and we started the optical fiber networks deployment commercially to transfer information across the Atlantic. But the deployed optical networks have one bottleneck i.e. they use optical fiber only for transmission of the signal and processing of signal takes place using electronic devices. Thus this optical to electronics domain and back to optical domain conversion (O-E-O) restricts optical networks to be utilized up to their full capacity.

As time is progressing, the world is quickly moving towards replacing electronics processing system by all optical processing system in optical networks such that optical signals can be processed without any requirement of O-E-O conversion. With this idea, researchers around the world began working on Photonic Integrated Circuits (PIC). The photonics integrated circuits are similar to their counterpart electronics integrated circuits. The major difference between the two is that the PIC works on optical wavelengths typically in the visible spectrum or near infrared 850 nm-1650 nm. A PIC is a platform that integrates many photonic components like optical filters, optical add-drop multipliers, modulators, optical switches, etc. that work directly on optical signals. Major elements of a PIC are an optical light source such as LASER/LED, a photodetector, optical interconnects and signal processing devices.

The true challenge that remains for the researchers today is to develop an optical processor that can be used for direct processing of the optical signals. Analogous to electronics signal processor, an optical signal processor will also consist of miniature

elements out of which the most important are the logic gates, combinational circuits, optical filters.

In this dissertation work all optical photonics devices based on optical ring resonator and combinational circuits based on MZI structure using Lithium Niobate are proposed and numerically simulated. The principle of operation of ring resonator is based on Kerr effect and that of MZI is based on Electro-Optic effect. All the proposed logic devices have a high output power for high logic and also provide high extinction ratio. The Proposed notch filter based on LNOI resonates at 1.5709 um and notch bandwidth is 3.8 nm. The LNOI based OADM is designed for a 200 GHz channel spacing WDM system. The results are in the acceptable limits of the required system i.e. the FSR required is 3.2 THz and FWHM is 100 GHz. This OADM is optimized and cascaded to realize the eight channel multiplexer & demultiplexer for DWDM system with 100 GHz channel spacing. The insertion loss at the drop port is maximum 1.2 dB and the Q-factor is 1636. It can be used as Multiplexer as well as Demultiplexer in 8 channel DWDM systems. The data rate is 10 Gbps and hence this PIC can be used in DWDM-GPON network to enhance the performance.

Proposed 3-bit gray to binary code convertor based on MZI structure is analyzed for output power at each output port that can be used for high and low logic respectively. The extinction ratio at all output ports is calculated and the minimum obtained is 19.6 dB. The insertion loss is found to be 0.02 dB at port 3 & 6 and 0.7 dB at port 1.

For 2x1 MUX using SOA-MZI switch based on reversible logic, all the input combinations are verified. The SOA-MZI switch is only the active element of the PIC of the multiplexer. The power consumption of the PIC is optimized by optimizing the output power of the SOA-MZI switch. The power consumption in MZI is optimal with interferometric arm length L=14000 um and width of waveguide W= 8 um.

Contents

List of Figures

List of Tables

Abbreviations

O-E-O	Optical Electrical Optical
PIC	Photonic Integrated Circuits
LASER	Light Amplification by Stimulated Emission of Radiation
LED	Light Emitting Diode
VLSI	Very Large Scale Integration
SOI	Silicon on Insulator
GaAs	Gallium Arsenide
InP	Indium Phosphide
SiO_2	Silicon dioxide or silica
AWG	Arrayed Waveguide Grating
Si_3N_4	Silicon nitride
LN	Lithium Niobate
EO	Electro-Optic
AO	Acousto-Optic
TO	Thermo-Optic
LNOI	Lithium Niobate on Insulator
WDM	Wavelength Division Multiplexing
MZI	Mach-Zehnder Interferometer
SOA	Semiconductor Optical Amplifier
MgO	Magnesium Oxide
Ti-LN	Ti-indiffused Lithium Niobate
FSR	Free Spectral Range
Q factor	Quality factor
FWHM	Full Width at Half Maximum
MUX	Multiplexer
DEMUX	Demultiplexer
DWDM	Dense Wavelength Division Multiplexing
FDTD	Finite Difference Time Domain

GPON	Giga-bit Passive Optical Networks
BCD	Binary Coded Decimal
BPM	Beam Propagation Method
TE	Transverse Electric
ER	Extinction Ratio
IL	Insertion Loss
CNOT	Controlled NOT Gate
BS	Beam Splitter
BC	Beam Combiner
NRZ	Non-Return to Zero
Gbps	Gigabits per second

Chapter 1

Photonics Integrated Circuits: Devices, Issues and Applications

Light as a method of communication has been used since ancient times. Smoke and fire signals, light houses, etc. are used as the means optical communication to pass their messages. As technology developed, new inventions were made in the field of optics and photonics. Today a large portion of the fields which are identified with innovation utilize optics and photonics in somehow. Research in the field of optical communication has developed at a fast pace. In recent years analysts have planned and built up a few sorts of optical fibers; thin strands of glass that can be used for high data rate transmission [1]. As the technology developed the performance of optical fibers improved and we started the optical fiber networks deployment commercially to transfer information across the Atlantic. But the deployed optical networks have one bottleneck i.e. they use optical fiber only for transmission of the signal and processing of signal takes place using electronic devices. Thus this optical to electronics domain and back to optical domain conversion (O-E-O) restricts optical networks to be utilized up to their full capacity [2].

As time is progressing, the world is quickly moving towards replacing electronics processing system by all optical processing system in optical networks such that optical signals can be processed without any requirement of O-E-O conversion. With this idea, researchers around the world began working on Photonic Integrated Circuits (PIC).

1.1 The photonics integrated circuits

The photonics integrated circuits are similar to their counterpart electronics integrated circuits. The major difference between the two is that the PIC works on optical wavelengths typically in the visible spectrum or near infrared 850 nm-1650 nm. A PIC is a platform that integrates many photonic components like optical filters, optical add-drop

multipliers, modulators, optical switches, etc. that work directly on optical signals. Major elements of a PIC are an optical light source such as LASER/LED, a photodetector, optical interconnects and signal processing devices. The PIC can be designed by using two different approaches i.e. hybrid and monolithic [3]. In hybrid approach, all the components of the PIC such as source, detectors, amplifiers, modulators, multiplexers etc. are separately designed on different substrates and then integrated together on a single chip. This approach has a limitation of space means the resulted PIC size. In monolithic approach, a single and bigger substrate is taken and all the components are designed and developed in parallel and hence no post assembly is required. As all the components are fabricated on identical substrates, it gives an advantage of compactness and thus much work is being today in present times to fabricate a PIC using monolithic approach.

Unlike electronics VLSI circuits where Silicon is the dominant material, system PICs have been fabricated using a variety of materials, including electro-optic crystals such as Lithium Niobate, Silica on Silicon, Silicon on insulator (SOI), various polymers and semiconductor materials like GaAs, InP, etc. which are used to make semiconductor lasers [4]. The different materials are used because they each provide different advantages and limitations depending on the application. For instance, Silica (SiO_2) based PICs have very suitable properties for passive photonic circuits such as AWG, Y-splitter, ring resonator, etc. due to their comparatively low losses and low thermal sensitivity. GaAs or InP based PICs are used for the direct integration of light sources and Silicon PICs enable co-integration of the photonics devices with transistor based electronic devices.

1.2 Silicon based PICs

Silicon Photonics is an important field of research which has gained much attention these days [5]. The main idea behind this platform is to use silicon and its compounds as a material to form channel waveguides to fabricate monolithic PIC. Silicon based fabrication technology has developed enormously in past decades. Photonic integrated circuits that use Silicon substrate to develop the photonic components will be benefitted from the already developed and matured fabrication facilities that are employed in electronics; hence this field is growing rapidly in research. In SOI based photonics devices, silicon and silicon compounds such as SiO_2 and Silicon Nitride (Si_3N_4) will work as the channel waveguide surrounded by a material with the lower refractive index as cladding [6].

The PICs fabricated based on SOI platform have low propagation loss but for fine tuning of refractive index, they consume more power. Moreover, silicon lacks second-order optical nonlinearity for active photonics and, at telecommunication wavelengths, third-order nonlinear silicon devices typically suffer from nonlinear absorptions [7]. Hence, they are mostly suited for the first order passive photonics devices.

1.3 Lithium Niobate based PICs

As the photonics circuits became more and more complex and compact, the need of technology developed Lithium Niobate as an alternative to Silicon as the substrate material. Lithium Niobate (LN) is a suitable material with many interesting properties for integrated photonics [8]. First, it is transparent from the ultraviolet to the infrared range (0.35 to 5.0 um) [9]. Optical gain can be achieved by doping LN crystals with rare earth elements, such as erbium to design the all optical amplifier [10]. A unique advantage is that its strong second-order nonlinear optical properties, such as electro-optic (EO), acousto-optic (AO), thermo-optic (TO), etc. [11]. The LN platform based many devices designed in past such as EO-modulators, all optical switches, all optical logic gates, all optical combinational circuits like half adder, full adder, code convertors, all optical filters, optical ring resonators, optical add drop multiplexers (OADM), beam-splitters, beam-combiners etc. [12-19].

The bending radius of LN based ring waveguides is more as compare to Silicon based as the refractive index contrast is less for LN channel waveguides. This is overcome by using the Lithium Niobate on Insulator (LNOI) platform. LNOI based devices provide good vertical and lateral refractive index contrast and mode confinement [20-22].

1.4 Application areas of photonics integrated circuits

The main application area of photonics integrated circuits [23] are listed below:

- Next-generation optical networks
- Optical interconnects
- Wavelength division multiplexed (WDM) systems
- Coherent transceivers
- Lab-on-a-chip
- Large-scale photonic integrated circuits (LS-PICs)

- Bio-photonics
- Optical sensors
- All optical signal processing

The true challenge that remains for the researchers today is to develop an optical processor that can be used for direct processing of the optical signals. Analogous to electronics signal processor, an optical signal processor will also consist of miniature elements out of which the most important are the logic gates, combinational circuits, optical filters.

In this dissertation work, some of the photonics devices based on Lithium Niobate platform are designed and simulated for photonics integrated circuits.

1.5 Organization of the Report

Chapter 1 gives a brief introduction to the photonics integrated circuits and various platforms for the development of the PICs. This chapter also gives a brief introduction about Silicon and Lithium Niobate photonics. The various application areas of PICs and some issues of photonics platforms also mentioned.

Chapter 2, a literature survey is carried out that consists of important properties of Lithium Niobate crystal and its development to become a perfect substrate material. The various diffusion methods are discussed to form the LN channel waveguides. The fabrication process of LNOI wafer is also described.

Chapter 3 gives an introduction to the optical ring resonator; fundamental component used in this work for the development of all optical signal processing devices. It's different configurations; all pass filter and add drop filter configuration are described. The notch filter and optical add drop multiplexer are designed and results are plotted.

Chapter 4 gives a detail insight in the working principle of the Mach-Zehnder Interferometer (MZI) and all optical XOR/XNOR logic gate based on MZI. The 3-bit gray to binary code convertor is designed using the MZI structure. The performance of the code convertor is also discussed.

Chapter 5 discusses the reversible logic and its importance to realize the low powered logic gates. Some of the reversible logic gates are discussed. A detail description of

the all optical 2x1 multiplexer based on semiconductor optical amplifier (SOA) MZI structure using reversible logic. The power analysis of MUX is also done to optimize the power consumption.

Chapter 6 summarizes the major results and concludes this dissertation work related to all optical devices based on Lithium Niobate for photonics integrated circuits. In chapter 7, future scope of this work is discussed.

Chapter 2

Lithium Niobate: A Perfect Substrate Material

All optical high speed and secure communication networks are growing in complexities and becoming mature day by day. The need of lower powered, ultra-high speed and smaller die size devices help the Lithium Niobate (LN) crystal to grow as a perfect choice for the substrate martial. With unique electro-optic (EO) properties of LN, it has been used to grow bigger wafer substrates that can exhibit small dielectric constant and can be used for fast device responses with low power consumption. Silicon photonics is well matured and stable technology, so Lithium Niobate on Insulator (LNOI) technology is developed to design the devices with low loss, compact in size and to utilize the silicon photonics advantages in the fabrication process. In this chapter, we will discuss the important properties of Lithium Niobate and its different variants that are used for different applications.

2.1 Lithium Niobate crystal

Lithium-Niobate crystal is a nonlinear, colorless, ferroelectric, and insoluble with water and it is used as substrate material for a variety of applications [11]. It shows an extensive electro-optic (EO), acousto-optic (AO), thermo-optic (TO) effects, which makes it suitable for cutting edge optics base material. In the EO and TO effect, the progressions in refractive index is incited by applying an electric field and temperature, while in the AO– effect, the change is brought on by interaction between acoustic and optical waves in the crystal. A genuine inconvenience of undoped $LiNbO_3$ is that it usually shows the so called ‘‘Optical Damage’’ [24] a sort of photorefractive effect when illuminated with high power laser beam of visible wavelength. This effect limits the stability of undoped LN crystal in nonlinear optical applications and Mg doped LN is used to compensate.

Some of the important specifications of LN crystal are tabulated in table 2.1. The most of the optical devices designed to at 1550 nm and 1300 nm as their center wavelength. The LN crystal shows appropriate physical and optical properties at these two wavelengths.

Table 2.1

Important specifications of LN crystal

Name	Value
Chemical formula	$LiNbO_3$
Crystal structure	Trigonal
Molecular weight (g/mol)	147.9
Density (g/cm^3) at 293 ^oK	4.644
Transmittance range (nm)	350-5500
Melting temperature (^oK)	1530
Curie temperature (^oK)	1415
Band gap (eV)	4.0
Optical damage threshold (MW/cm^2)	250@1064 nm, t ~ 10 nsec,
Refractive indices	$n_e = 2.138$, $n_o = 2.211$ @ 1550 nm $n_e = 2.146$, $n_o = 2.220$ @ 1300 nm $n_e = 2.156$, $n_o = 2.322$ @ 1064 nm
Electro-optic coefficients (pm/V)	r^T_{33}=32,r^S_{33}=31,r^T_{31} = 10,r^S_{31} = 8.6 r^T_{22} = 6.8, r^S_{22} = 3.4

The wafer of LN crystal is prepared by providing the different cuts like x-cut, y-cut and z-cut. The sectional view of the lithium Niobate optical wafer is shown in figure 2.1. Table 2.2 contains the properties of the commonly used LN wafers.

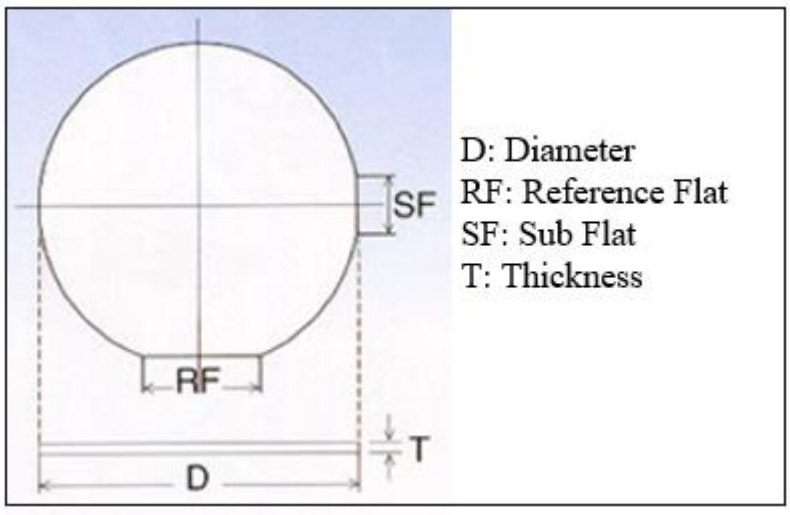

Fig. 2.1 The sectional view of the optical wafer of the Lithium Niobate.

Table 2.2

Physical orientation of the commonly used LN crystals

Orientation	Reference flat perpendicular to	Sub Flat	Sectional view
Z-cut	Y	-X	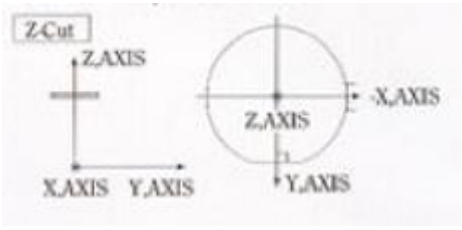
Y-cut	Z	+X	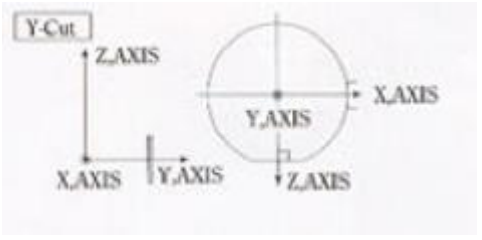
X-cut	Z	-Y	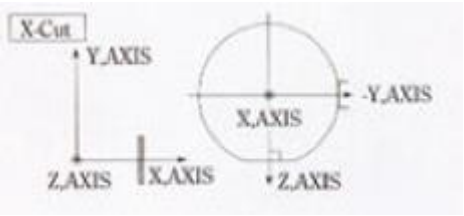

2.2 Diffusion in LN to form channel waveguides

Different dopants like Magnesium Oxide (MgO), Titanium (Ti), etc. [25] are used to dope in the LN substrate to form channel waveguides. The EO–switches and modulators are fabricated with either Ti-indiffusion or annealed proton exchange process. In another case, where optical spillage should be stayed away, MgO is utilized to shape Mg diffused LN channel waveguide.

2.2.1 Ti-indiffusion process

Photolithography process is used for selective diffusion of Titanium [26]. The generic steps for the photolithography process are shown in figure 2.2. The indiffusion of Ti is carried out by depositing a Ti–strip of fixed thickness and width onto LN substrate followed by heating in a controlled environment. After the process, the Ti–ions are able to penetrate the LN substrate and form a bell shaped index pattern. The Titanium doped LN (Ti-

LN) waveguide possesses a graded index profile which is characterized by diffusion constant, temperature and temperature coefficient. The optical loss of a conventional Ti-LN waveguide modulator is usually 0.2 dB/cm.

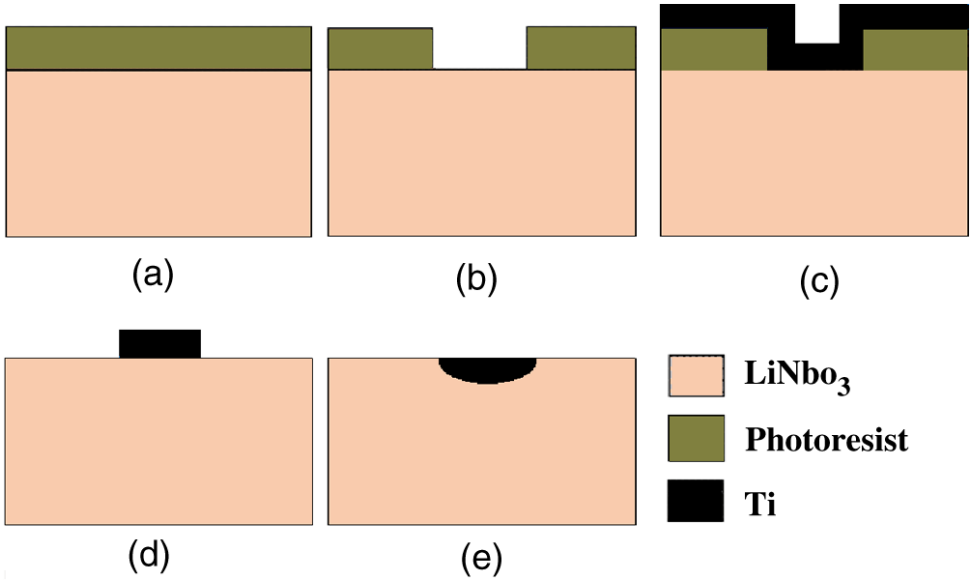

Fig. 2.2 Generic process steps for Ti–indiffusion within Lithium Niobate substrate.

2.2.2 Proton exchange process

The process of proton exchange in LN includes substitution of Lithium ions (Li^+) by Hydrogen ions or protons (H^+) under specific process environment [27-28]. It results in refractive index change, thus forming waveguide which has two stages:

- Basic proton exchange from an organic proton source
- Annealing post processing

Basic proton exchange includes the immersion of LN substrate in an appropriate proton source, commonly used proton source is Toluic acid or Benzoic acid and then heating for a couple of hours at temperatures ranging from 150 ^oC to 300 ^oC. The annealing post processing involves solely heating of the sample and a redistribution of the Lithium and Hydrogen ions takes place. The refractive index distribution is strongly dependent on the post–exchange time and the post–exchange temperature. The process of proton exchange to form the LN channel waveguides is shown in figure 2.3.

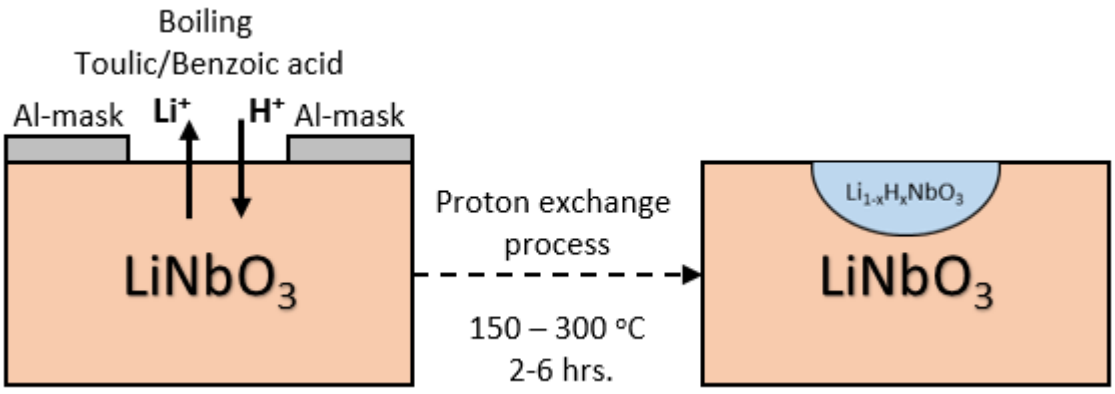

Fig. 2.3 Proton exchanged process within LN substrate.

2.2.3 Magnesium diffusion process

Magnesium doping can improve the stability of Lithium-Niobate ($LiNbO_3$) crystal in non-linear optical applications. Magnesium Oxide (MgO) is mainly used as Mg source to form Mg:$LiNbO_3$ [29]. The negative index changes in the base material are observed i.e. both the ordinary (n_o) and the extraordinary (n_e) refractive index decrease due to the Mg diffusion.

2.3 Lithium Niobate on Insulator (LNOI)

The crystal ion slicing combined with wafer bonding can realize high index contrast LN on insulator (LNOI) waveguides with submicron core size [20]. Therefore, LNOI can be a good candidate for various integrated functional optical devices. Ridge waveguides and photonic wires are fabricated in LNOI and their applications such as modulators or microring resonators have been reported. The LNOI wafer is prepared by using the different methods like chemical vapor deposition, RF sputtering, molecular beam epitaxy, etc. [30-32]. However, all of these methods face some difficulty in producing high crystalline quality materials.

2.3.1 Smart-Cut method for fabrication of LNOI wafer

In this method, the high-dose implantations of H^+ and/or He^+ ions are used for cleaving single-crystalline ferroelectric thin films from a bulk material. The process to fabricate the LNOI wafer is divided into two major parts as following:

1. Crystal ion slicing
2. BCB bonding or Crystal bonding to SiO_2

The full wafer fabrication process is schematically shown in figure 2.4. At first, a Z-cut LN wafer is implanted by He-ions with a high dose forming an amorphous layer at a depth dependent on the implantation energy. Another Z-cut LN sample is coated by a SiO_2-layer. Now, these two samples are bonded together either using BCB bonding or crystal bonding to the SiO_2. The mostly used bonding is SiO_2 bonding with crystal as compared to the BCB bonded material, annealing at much higher temperatures are possible in SiO_2 bonded material. This is important to retain EO and nonlinear properties of the thin LN film. Also, high temperature annealing significantly reduces the surface roughness.

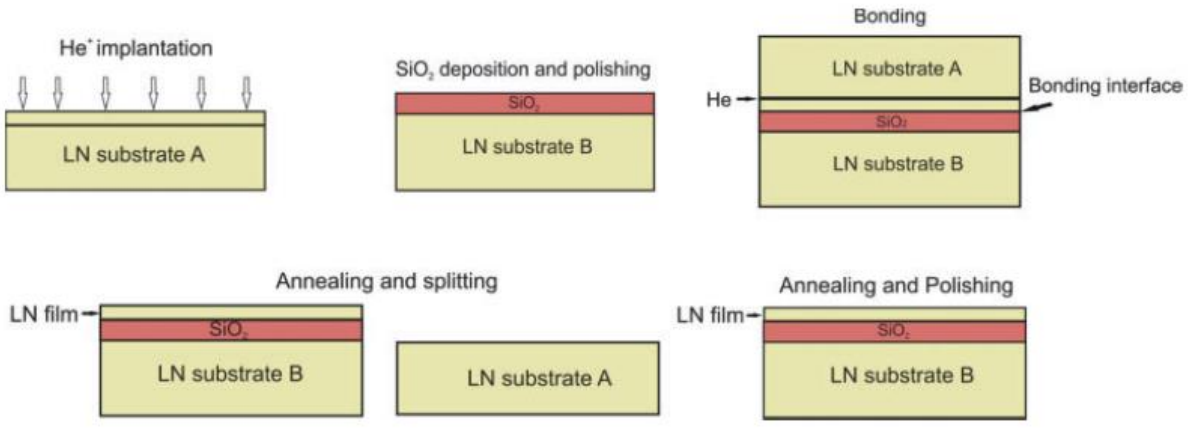

Fig. 2.4 Fabrication scheme of LNOI [20].

In this dissertation work all the devices are designed using the Lithium Niobate substrate. The optical add drop multiplier and notch filter are designed over the Lithium Niobate on Insulator platform. The gray to binary code convertor and 2x1 MUX are designed using the Ti-indiffused LN channel waveguides.

Chapter 3

Optical Ring Resonator based Optical Add Drop Multiplexer

The optical ring resonator is mainly used in all pass filter configuration or add-drop filter configuration when coupled with external waveguides. The most common coupling mechanism is using co-directional evanescent coupling between the ring and an adjacent bus waveguide. As will be discussed in more detail in the next section, the transmission spectrum of the bus waveguide with a single ring resonator will show dips around the ring resonances. This way, the ring resonator behaves as a spectral filter, which can be used for applications in optical communication, especially wavelength division multiplexing (WDM). When one more bus waveguide is coupled on another side to collect the resonant wavelength at drop port then it works as optical add drop multiplexer.

3.1 Optical Ring Resonator: Theory and Principle

The simplest optical ring resonator consists of a straight waveguide and a ring waveguide [33-34]. The two waveguide cores are placed close to each other, so light coupled from one waveguide to the other. When the length of the ring waveguide is an integer number of wavelength, the ring waveguide is resonant to the wavelength and the light power stored in the ring builds up.

The wave transmitted through the straight waveguide is the interference of the incident wave and the wave that couples over from the ring to the straight waveguide. Schematically, you can think of the ring resonator as shown in figure 3.1 below. A part of the incident wave E_{i1} is transmitted in the straight waveguide, whereas a fraction of that field couples over to the ring. Similarly, some of the light in the ring couples over to the straight waveguide, whereas the rest of that wave continuous around the ring waveguide.

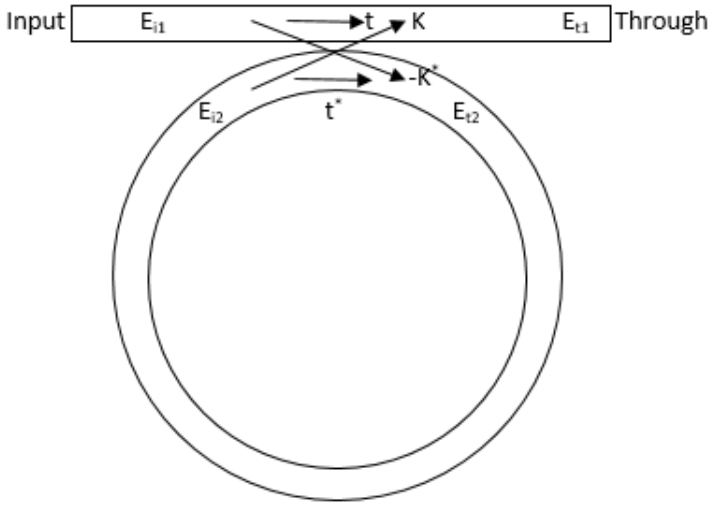

Fig. 3.1 Schematic of an optical ring resonator in all pass filter configuration.

The transmitted fields are related to the incident fields through the matrix-vector relation as given below:

$$\begin{bmatrix} E_{t1} \\ E_{t2} \end{bmatrix} = \begin{bmatrix} t & k \\ -k^* & t^* \end{bmatrix} \begin{bmatrix} E_{i1} \\ E_{i2} \end{bmatrix} \tag{3.1}$$

Where

E_{i1} and E_{i2} are the incident fields,

E_{t1} and E_{t2} are the transmitted/coupled fields,

t is the transmission coefficient,

k is the coupling coefficient.

The matrix elements are such that the total input power is equal to the total output power and the sum of the squares of the transmission and coupling coefficients is unity. So, we can define the wave propagating through waveguide by using eq. 3.4.

$$|E_{i1}|^2 + |E_{i2}|^2 = |E_{t1}|^2 + |E_{t2}|^2 \tag{3.2}$$

$$|t|^2 + |k|^2 = 1 \tag{3.3}$$

$$E_{i2} = E_{t2} L e^{-i\emptyset} \tag{3.4}$$

Where L is the loss coefficient for the propagation around the ring and $\emptyset$ is the accumulated phase. The transmission coefficient, t can be separated into transmission loss |t| and the corresponding phase $\emptyset_t$ as

$$t = |t|e^{-i\emptyset_t} \tag{3.5}$$

Combining equation 3.1 to 3.5, the transmitted field can be written as

$$E_{t1} = \frac{|t| - Le^{-i(\emptyset - \emptyset_t)}}{1 - |t|Le^{-i(\emptyset - \emptyset_t)}} E_{i1} e^{-i\emptyset_t} \tag{3.6}$$

At resonance, when ($\emptyset$ - $\emptyset_t$) is an integral multiple of 2π, and |t| = L, the transmitted field is zero. The condition that |t| = L is called critical coupling. Thus, when the coupler's transmission loss balances the loss for the wave propagating around the ring waveguide you get the optimum condition for a band-stop filter, a notch filter [35-36].

Another configuration that is primarily used is the add drop filter configuration as shown in figure. 3.2. Equations (3.1) to (3.6) mentioned above hold true for add drop filter configuration also [37]. It is a four port device consist of input, through, add and drop ports.

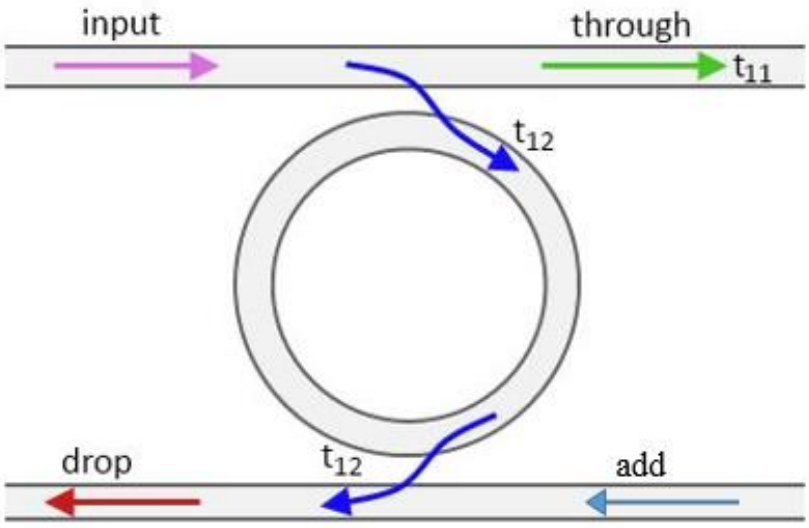

Fig. 3.2 Optical ring resonator in add-drop filter configuration.

Optical signals can be derived at the input or the add port and the output can be obtained at the through port or the drop port. When the wavelength multiplexed signal is given at the input port of the OADM, the wavelength that matches the resonant wavelength of the ring resonator is reached at the drop port and other wavelength signals are collected at through port. Proper design of the OADM results in zero transmission at the resonance and maximum power is coupled to the drop port. Hence the OADM can work as the multiplexer or demultiplexer for the DWDM networks.

The dropped optical power, P_{drop} is calculated in terms of input power, P_{in} and coupling coefficients, t_{11} & t_{12} as

$$P_{drop} = P_{in} \frac{|t_{12}|^4}{\left|1 - t_{11}{}^2 e^{j\beta L}\right|^2} \tag{3.7}$$

Where

P_{drop} and P_{in} are the power at drop and input ports,

t_{11} and t_{12} are the coupling coefficient,

β is the phase constant,

L is the effective length of the ring.

At the resonance the phase difference after a round trip is integer multiple of 2π i.e. $\beta L = 2\pi m$, where m is mode number. The effective length depends on the refractive index of the material and is defined as $L = m\lambda_0/n_{eff}$, where the effective refractive index is defined as $n_{eff} = c\beta/\omega$ and $\lambda_0 = c/f_0$ is the free-space wavelength at the resonance frequency f_0. The effective refractive index also depends on the free spectral range (FSR) i.e. the spacing between the resonant wavelengths. The FSR can be explained in terms of effective length of ring and the group refractive index, $n_g = c(d\beta/d\omega)$ as

$$FSR = \frac{\lambda^2}{n_g L} \tag{3.8}$$

The Q-factor of the resonant circuit is a figure of merit which measures the quality of the circuit. The higher value of Q-factor is needed for filter applications. The Q-factor can be calculated as the ration of resonant wavelength and full width at half maximum (FWHM).

$$Q = \frac{\lambda_{res}}{2\partial\lambda} = \frac{n_g L\pi}{\lambda} \frac{|t_{11}|}{1-|t_{11}|^2} \tag{3.9}$$

Add drop filter configuration of optical ring resonator is widely used in photonic integrated circuits to develop on chip MUX/DEMUX [38-39]. In this dissertation work, add drop filter configuration is employed to develop all optical add drop multiplex for DWDM networks.

3.2 Optical Notch Filter

The Optical Notch Filter is important in all optical communication networks for optical signal processing. In this section, we have reviewed structuring of an all optical notch filter using the microring resonator based on Lithium Niobate on Insulator (LNOI) platform. The electromagnetic waves and beam envelopes physics interfaces are utilized to handle the propagation over distances that are many wavelengths long with scattering boundary conditions. The proposed notch filter shows almost zero transmittance at resonance and the notch bandwidth is found as 3.8 nm. The proposed structure is suitable for ultra-fast optical communication networks.

3.2.1 Design layout of Notch Filter

The design parameters of the optical ring resonator based Notch filter are given in table 3.1. The 2-D model is designed and simulated using the COMSOL tool. In this model core is made up of Lithium Niobate and SiO_2 is used as the cladding material.

Table 3.1

Design Parameters of Ring Resonator

Name	Value	Description
W_core	0.20 um	Core width
W_clad	2.00 um	Cladding width
R_0	7.053 um	Radius of curvature
N_core	2.211	LN refractive index
N_clad	1.444	SiO_2 refractive index
Dx	0.72 um	Separation between waveguides

The ring resonator is designed using the equations defined in section 3.1. The center wavelength is 1550 nm. The Y-cut Lithium Niobate crystal is used to design the channel waveguide. The design layout is shown in figure 3.3. The separation between the bus waveguide and ring waveguide i.e. the coupling gap is 720 nm. The radius of the ring waveguide is 7.053 um. The width of the core waveguide is 200 nm.

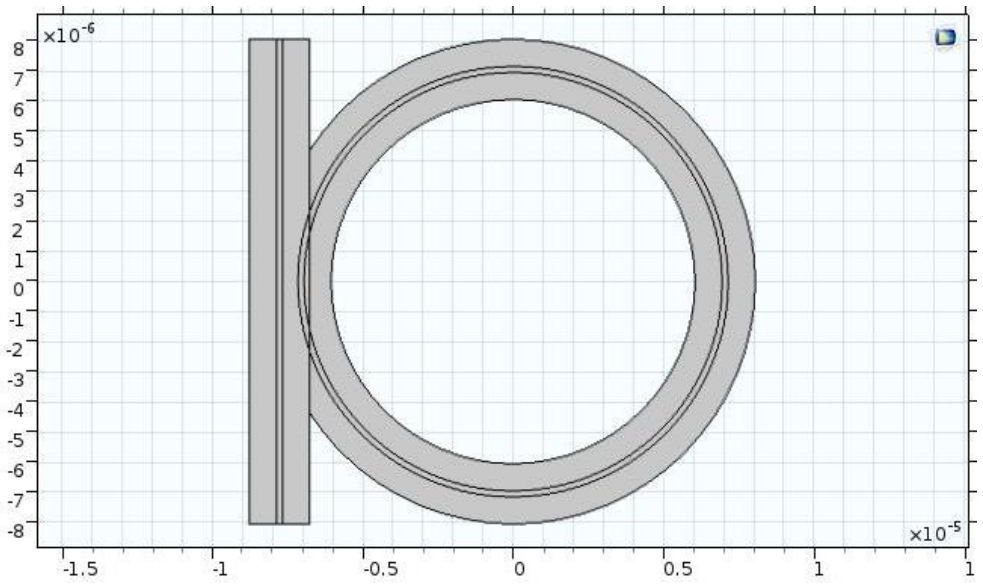

Fig. 3.3 Design layout of ring resonator notch filter.

3.2.2 Simulation results and discussion

The electric field distribution along the ring resonator is shown in figure 3.4 and figure 3.5. At resonance, the electric field intensity is almost zero at the output port and at a non-resonating wavelength, the electric field intensity received at output port is nearly equal to the incident field.

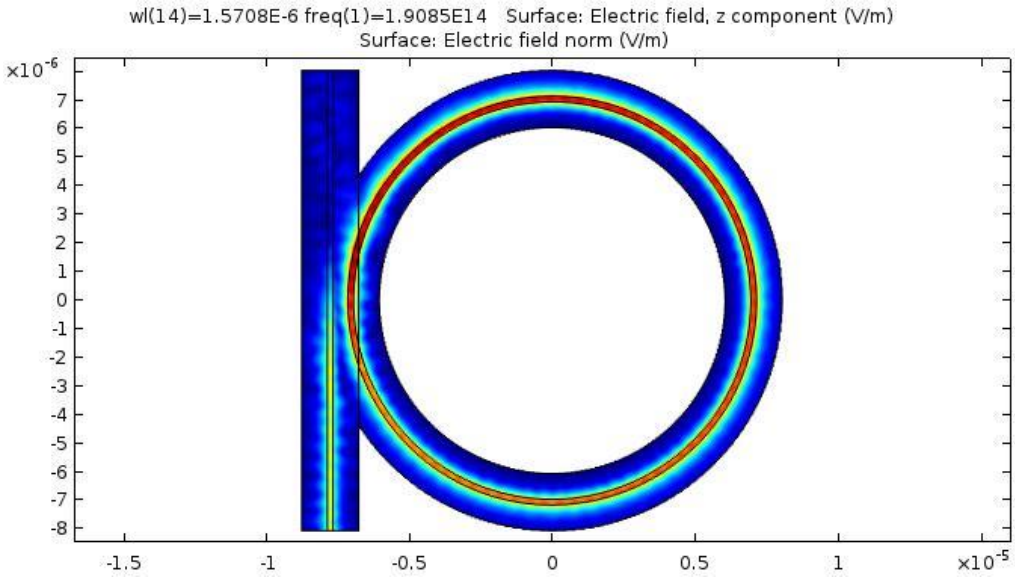

Fig. 3.4 E-Field distribution at resonant wavelength.

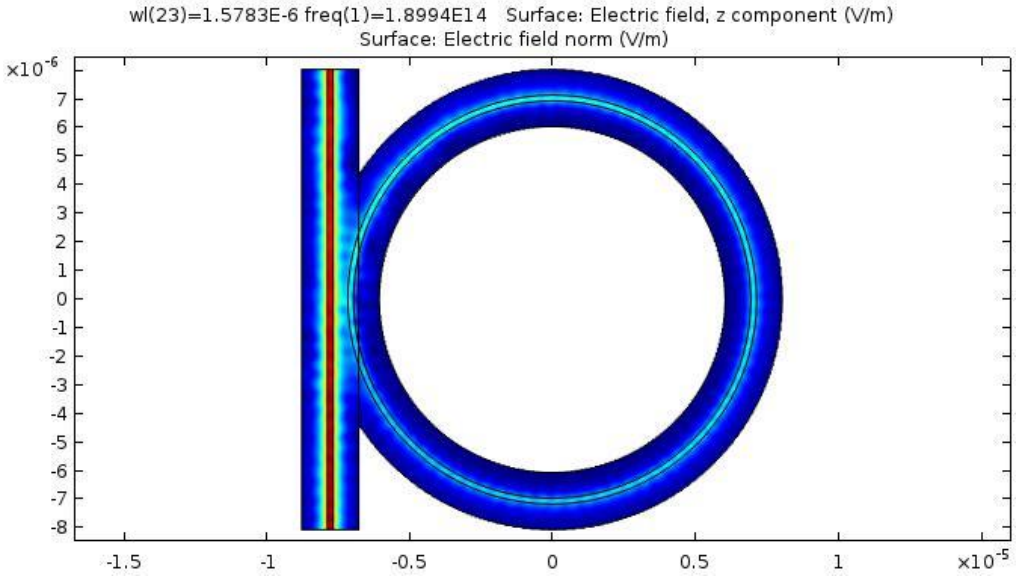

Fig. 3.5 E-Field distribution at non-resonant wavelength.

The transmittance curve at the output port is drawn for the Notch Filter using LNOI as shown in figure 3.6. It can be seen from the transmittance curve that the Notch filter has zero transmittance at resonating wavelength and has more than 90% transmittance at non-resonating wavelengths. The Notch Bandwidth is 3.8 nm at the resonating wavelength of 1.5709 um. The Q-factor of the Notch filter based on LNOI is 415.

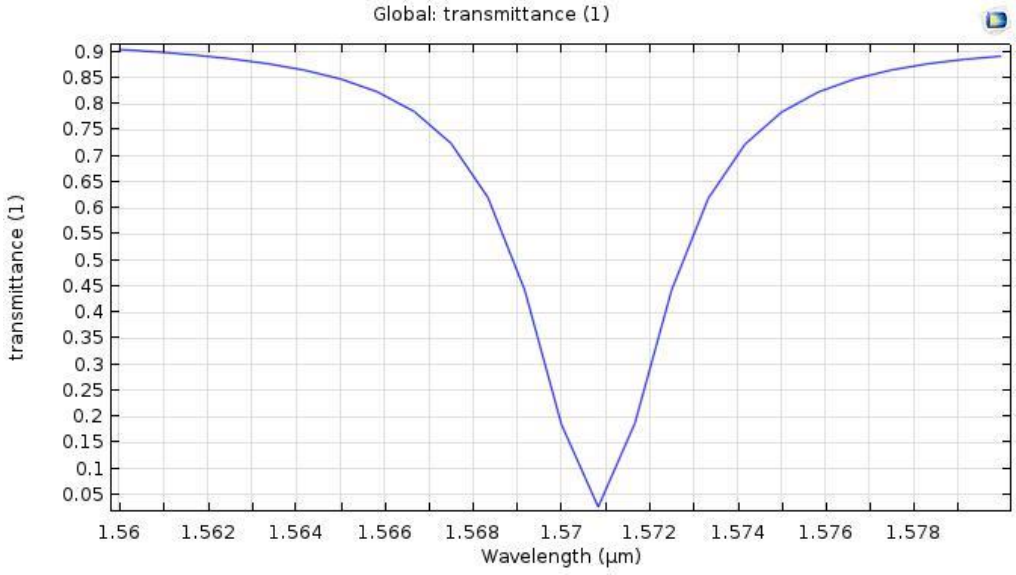

Fig. 3.6 Transmittance curve of notch filter based on LNOI.

An optical notch filter can be used to filter out the specific wavelengths and it is mainly used in optical signal processing and optical biosensors. The notch bandwidth of the

optical ring resonator based notch filter is 3.8 nm and possesses almost zeros transmittance at resonant wavelength. Q-factor is calculated as 415, which can be improved further as well.

3.3 Optical add drop multiplexer

The OADM is designed using the optical microring resonator using the Lithium Niobate on Insulator (LNOI) channel waveguides. LNOI possesses high refractive index contrast and also depicts better electro-optic & acousto-optic effects. The finite difference time domain (FDTD) method is used to calculate the performance of the proposed device. It is suitable for a WDM system with channel spacing of 200GHz.

3.3.1 Design implementation of the OADM

The OADM is designed based on optical ring resonator for the WDM system with a channel spacing 200 GHz (1.6 nm at 1550 nm) and we wanted to drop every 16th channel i.e the required free spectral range (FSR) is 3.2 THz. The required FWHM is 100 GHz that corresponds to high Q-factor. The layout of design is shown in figure 3.7. The substrate is Lithium Niobate then a thin layer of SiO_2 on which OADM is designed. The waveguide width is 700 nm and height is 350 nm. The radius of the ring is 5.78 um.

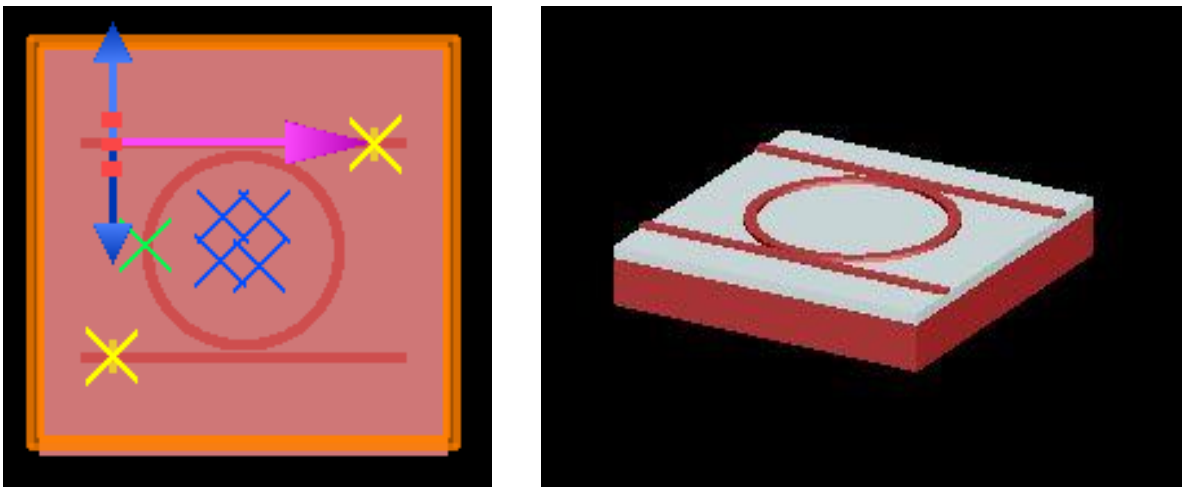

Fig. 3.7 Design layout of OADM: (a) Top view and (b) 3-D view.

The design parameters are described in table 3.2. Each microring is designed using Lithium Niobate as substrate then a thin layer of SiO_2 on which OADM is designed using Lithium Niobate channel waveguide. The waveguide width is 700 nm and height is 350 nm. The separation between the bus waveguide and ring waveguide is 100 nm. The refractive

index of LN and SiO2 is taken at 1.55 um. The fundamental mode is confined in the waveguide as shown in figure 3.8. The mode is confined means that the optical signal is propagating through the waveguide core and leakage signal is less. The TE polarization is used in simulation.

Table 3.2

Design Parameters of the optical add drop multiplexer.

Name	Value	Description
W_core	700 nm	Waveguide width
H_core	350 nm	Waveguide height
R_0	59.7 um	Radius of curvature
N_core	2.211	LN refractive index
N_clad	1.444	SiO_2 refractive index
Dx	100 nm	Separation b/w Waveguides

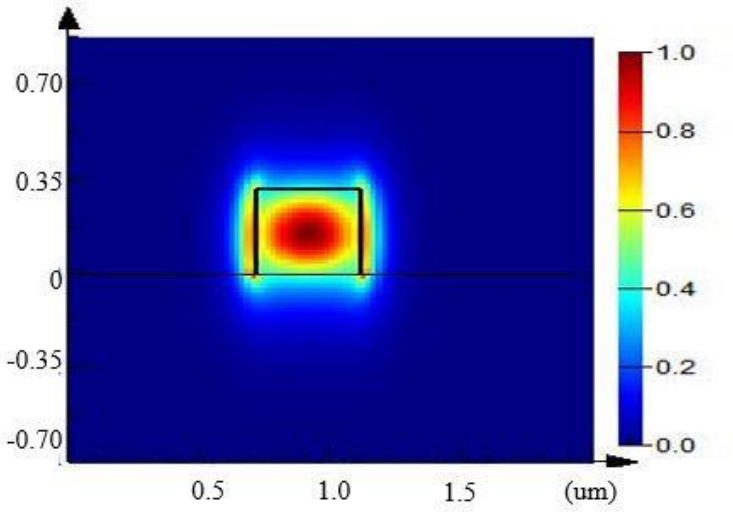

Fig. 3.8 Fundamental mode of propagation in channel waveguide.

3.3.2 Simulation results and discussion

The design of OADM is simulated using FDTD method. The transmission curve is observed at through port and drop port and plotted in figure 3.9. The simulation results are compared with the theoretical results and plotted in figure 3.10. It would be seen that the results are in quite matching in terms of FSR but not in terms of Q-factor. The reason is that

all the sources of losses are ignored in theoretical curve calculations.

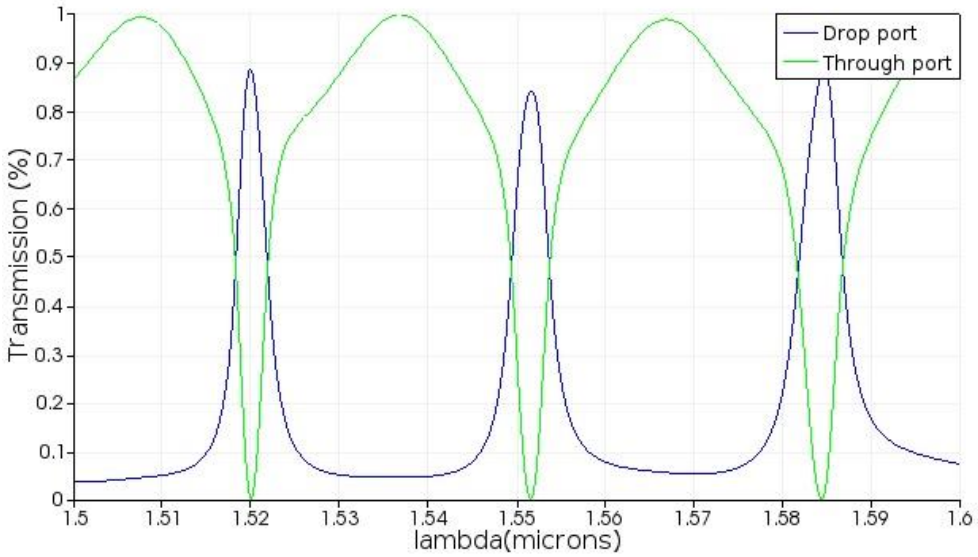

Fig. 3.9 Transmission plot at drop and through port.

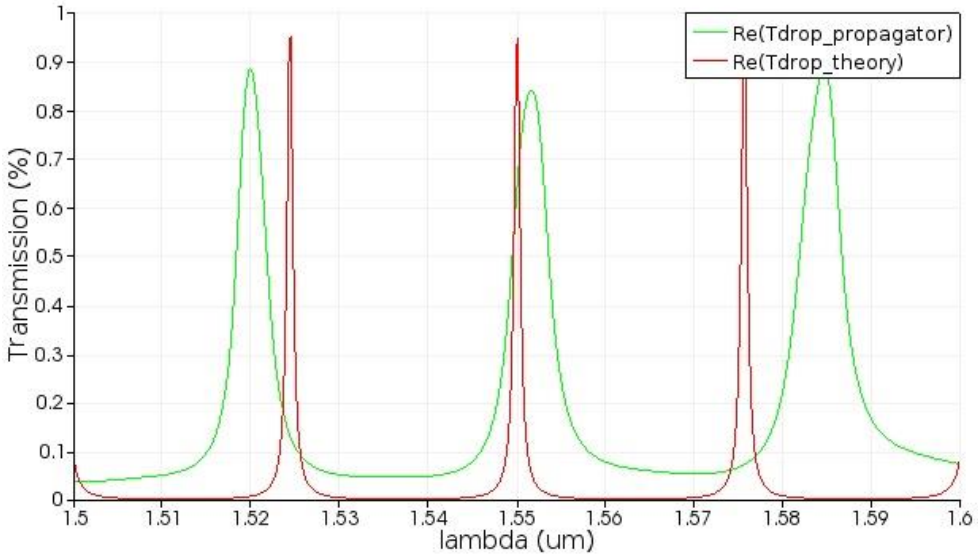

Fig. 3.10 Theoretical and propagator drop port transmission curve.

In this section, the structuring of all optical add drop multiplexer based on microring resonator is done by using the Lithium Niobate waveguide on insulator (LNOI). The OADM is designed for a 200 GHz channel spacing WDM system. The results are in the acceptable limits of the required system i.e. the FSR required is 3.2 THz and FWHM is 100 GHz. This device can be cascaded to form router which is an essential part of all optical communication system. Also by using the electrodes the proposed OADM can be made tunable.

3.4 Eight channel OADM

The ring resonators are cascaded to make all optical multiplexer and demultiplexer for DWDM systems. Eight microring resonators based on LNOI are cascaded to form the PIC of eight channel OADM. The block diagram of 8 channel OADM using microring resonator is shown in figure 3.11; each consists of two bus waveguide which is coupled to a ring waveguide. It is a four port device, for demultiplexer we are using input port, through port and drop port and for multiplexer input port, through port and add port is used.

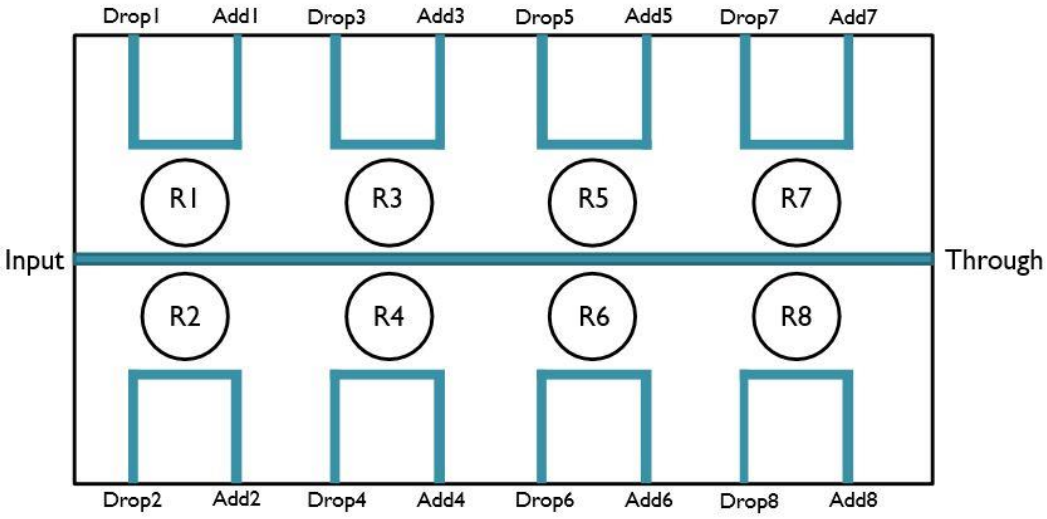

Fig. 3.11 The block diagram of 8 channel OADM.

3.4.1 Design implementation of the 8 channel OADM

The PIC of eight channel OADM based on optical ring resonator is designed for the DWDM system with a channel spacing 100 GHz (0.8 nm at 1550 nm) and we wanted to drop every 8th channel i.e. the required free spectral range (FSR) is 800 GHz (6.4 nm). The layout of design is shown in figure 3.12. The radius of ring is 59.7 um hence effective length L= 375 um.

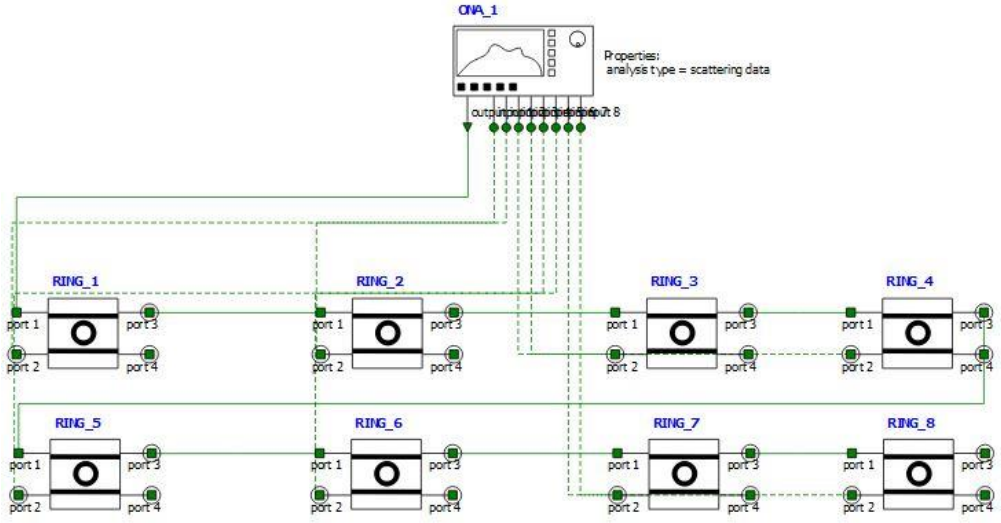

Fig. 3.12 Design Layout of PIC of 8-channel OADM.

3.4.2 Simulation results and discussion

The OADM designed using LNOI and simulated using FDTD method. The PIC is simulated on the Lumerical Interconnect tool using the scattering data analysis. The transmission curve is observed at drop port of each ring and plotted in figure 3.13. It is observed the insertion loss at the drop port is maximum 1.2 dB when used as demultiplexer and the Q-factor is 1636. The data rate is 10 Gbps. The crosstalk is also minimal and at the resonate condition optical power at other ports is zero.

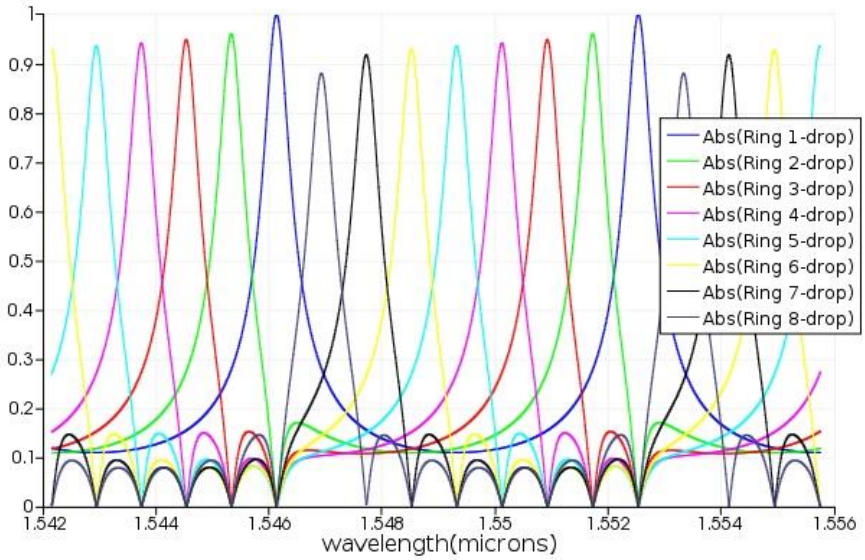

Fig. 3.13 Transmission plot at drop port of each ring.

The transmission plot at the through port of 8-channel OADM as DEMUX when four channels are dropped and at the through port of 8-channel OADM as MUX when those 4 channels are added again is shown in figure 3.14.

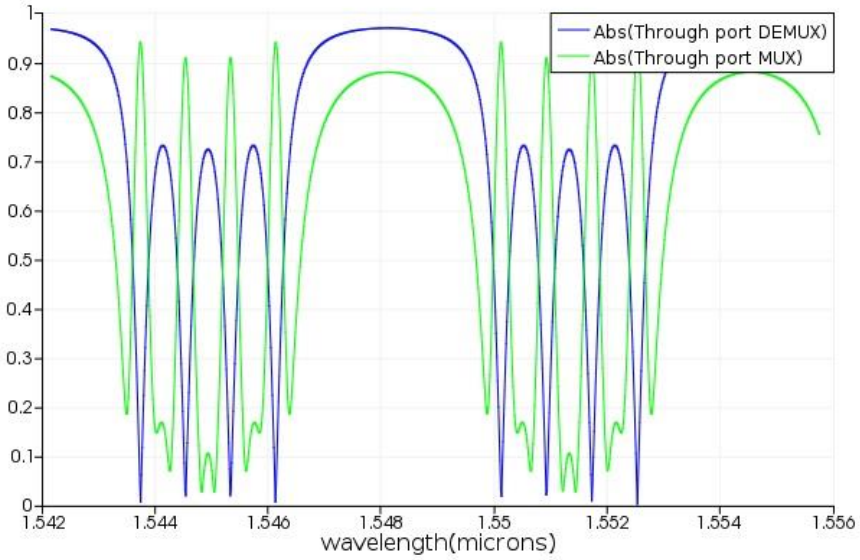

Fig. 3.14 Transmission plot at through port of DEMUX and MUX.

The PIC of 8 channel OADM can be used as Multiplexer as well as Demultiplexer in 8 channel DWDM systems. The data rate is 10 Gbps and hence this pic can be used in DWDM-GPON network to enhance the performance.

Chapter 4

MZI based Gray to Binary Code Convertor

All optical code converters are the essential circuits for secure optical digital communication like binary to gray, gray to binary, and gray to BCD code converters. In this dissertation work, electric gray to optical binary code converter using Ti-indiffused Lithium Niobate (Ti-LN) based Mach-Zehnder Interferometer (MZI) is designed and simulated. The MZI structure has been used to design the XOR logic gate [40], which is the elemental building block for the proposed gray to binary code converter.

4.1 Working principle of MZI

The Mach-Zehnder Interferometer is a highly configurable all optical device. It can be used as electro-optic modulator or all optical switch. The MZI structure, when used as EO-switch, consists of a 3-dB coupler at input side which works as beam-splitter, two parallel interferometric arms and second 3-dB coupler the output side which works as beam-combiner. The schematic diagram of the simple EO-switch based on MZI is shown in figure 4.1.

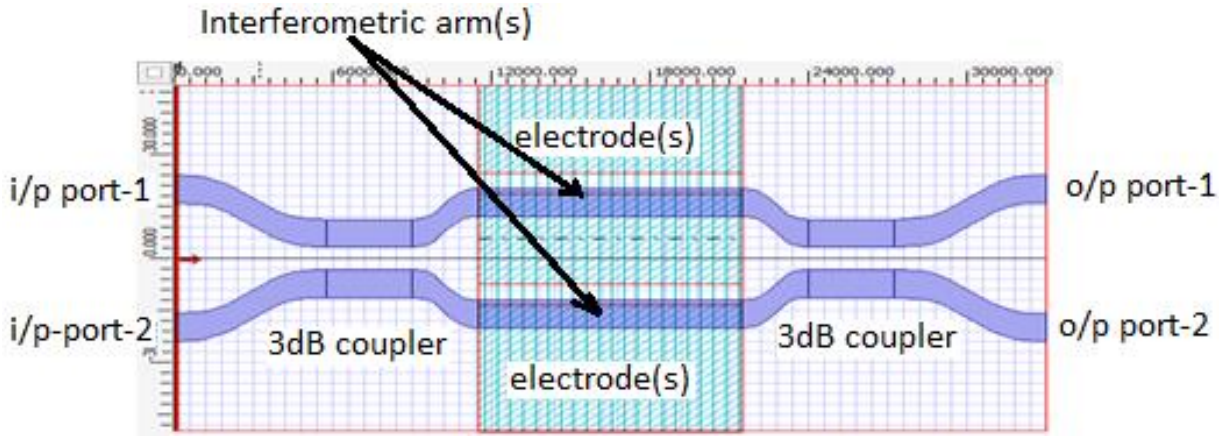

Fig. 4.1 Schematic view of Mach-Zehnder Interferometer.

The switching action takes place based on the relative phase change between the interferometric arms. The relative phase shift and the output power at port 1 & 2 can be calculated as:

$$P_{out1} = P_{in}\, sin^2 \frac{\Delta\emptyset}{2} \tag{4.1}$$

$$P_{out2} = P_{in}\, cos^2 \frac{\Delta\emptyset}{2} \tag{4.2}$$

$$\Delta\emptyset = \frac{\pi}{V_\pi} V \tag{4.3}$$

Where

P_{out1} and P_{out2} are the power at output ports,

P_{in} is the input power derived at the input port-1,

$\emptyset$ is the phase difference,

V is the electrode voltage and $V\pi$ is the electrode voltage corresponds to $\Delta\emptyset = \pi$.

When switching voltage V is zero switch operates in cross state i.e. P_{out2} is equal to the input power as the phase difference is zero and when switching voltage is equal to Vπ i.e. 6.75 V, switch will work in bar state i.e. output power is received at output port-1 as $\Delta\emptyset = \pi$ that corresponds the output power at output port-2 is zero.

4.2 Gray to Binary code conversion

The gray code is widely used in communication system as it a unit distance code i.e. the logic distance between any two consecutive codewords is one [41]. The mostly digital processing is done on binary codes. Hence, for doing the all optical signal processing we need all optical gray to binary code convertor. The 3-bit gray code can be converted into 3-bit binary code using the truth table given in Table 4.1. The output binary code bits are B2, B1 & B0 and the input gray code bits are G2, G1 & G0. The logical expression for the B2, B1 & B0 in terms of G2, G1 & G0 can be calculated by using the K-map as given below:

$$B2 = G2 \tag{4.4}$$

$$B1 = G2 \oplus G1 \tag{4.5}$$

$$B0 = G2 \oplus G1 \oplus G0 \tag{4.6}$$

Where,

The symbol $\oplus$ denotes the XOR logic operation.

Table 4.1

Truth table for the gray to binary conversion.

Gray Code			Binary code		
G2	G1	G0	B2	B1	B0
0	0	0	0	0	0
0	0	1	0	0	1
0	1	0	0	1	1
0	1	1	0	1	0
1	0	0	1	1	1
1	0	1	1	1	0
1	1	0	1	0	0
1	1	1	1	0	1

4.3 Implementation of code converter

The electric gray to optical binary code converter is designed using Ti-indiffused LN waveguide. The basic logic circuit in this code converter is the XOR gate which is designed using the MZI structure. The two input optical XOR/XNOR gate is designed by cascading two MZI switches. The design layout of 2-input XOR/XNOR gate is shown in figure 4.2, A and B are the logical inputs which are represented as the electrode voltage.

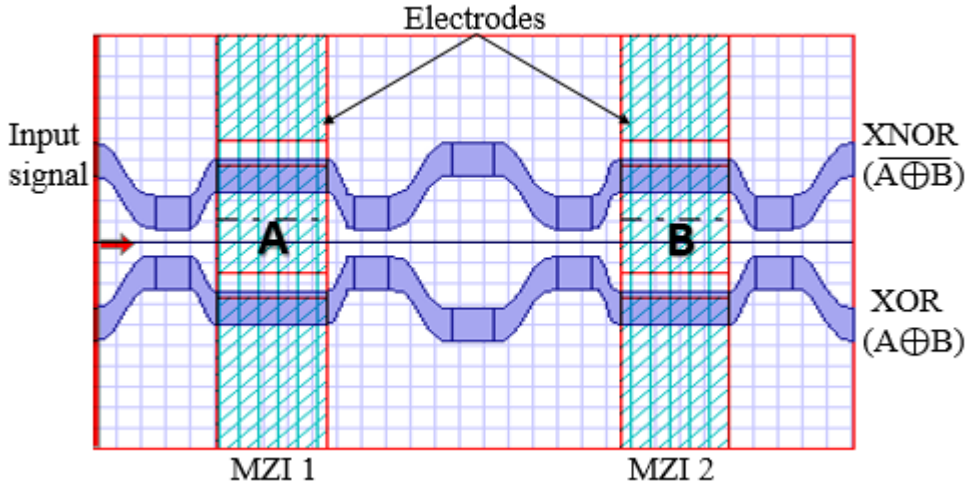

Fig. 4.2 Schematic view of 2-Input XOR/XNOR logic gate using MZI.

The output of the XOR gate is high when either of the input is high and it is low when either both are low or both are high. Here, logic inputs A & B are the electrode voltage i.e. zero corresponds to the logical zero and switching voltage corresponds the logical one. Hence, the 3-input XOR gate can be implemented by cascading the 3 MZI switches. The gray to binary code convertor is designed on Opti-BPM tool and the design is shown in figure 4.3 that consists of 6 MZI switches. The optical source is connected at 3 input ports and 6 output ports where the optical signal is received in which port 1, 4 & 5 corresponding to binary output B0, B1 & B2 and port 2, 3 & 6 gives the complementary binary outputs. Gray code inputs are given as the electrode voltage.

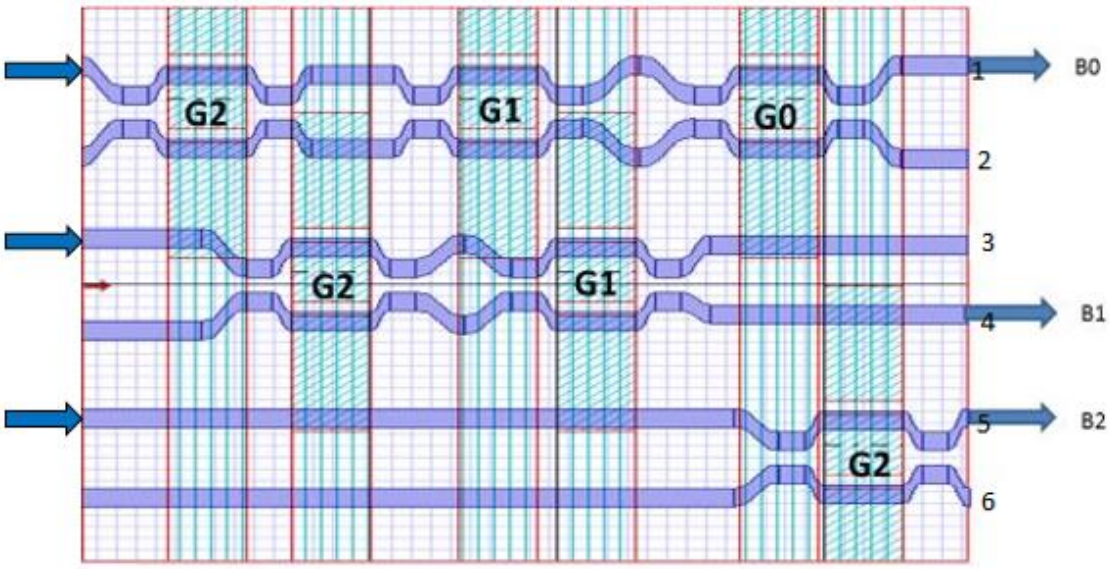

Fig. 4.3 The design structure of 3-bit gray to binary converter.

The waveguide width is 10um and material is Ti-LN with Titanium diffusion depth is 0.05um. The simulation wavelength used is 1.55um and polarization of the input optical signal is transverse electric (TE). At the input ports same optical source is used to drive the optical signal at input port 1, 3 & 5. The gray code inputs G2, G1 & G0 are represented by the electrode voltage where 0V is the logical zero and switching voltage 6.75V is equivalent to the logical 1.

4.4 Simulation results and waveforms

The layout is simulated using beam propagation method and all the combinations of truth table given in table 4.1 are verified. The waveforms of all eight combinations for 3-bit gray to binary code converter is shown in figure 4.4.

G2=0 G1=0 G0=0

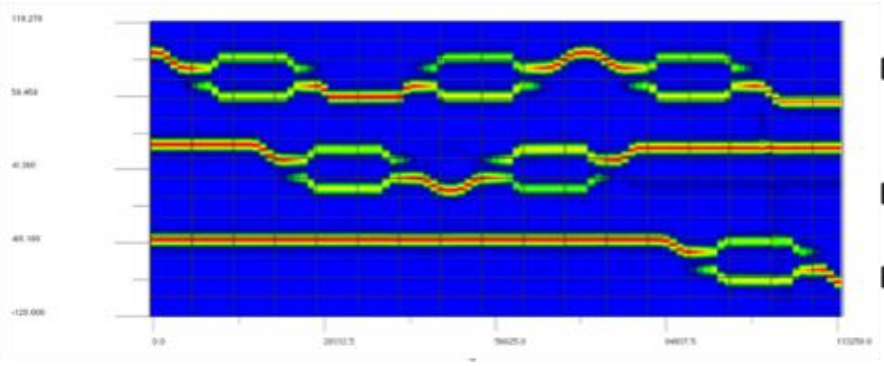

G2=0 G1=0 G0=6.75

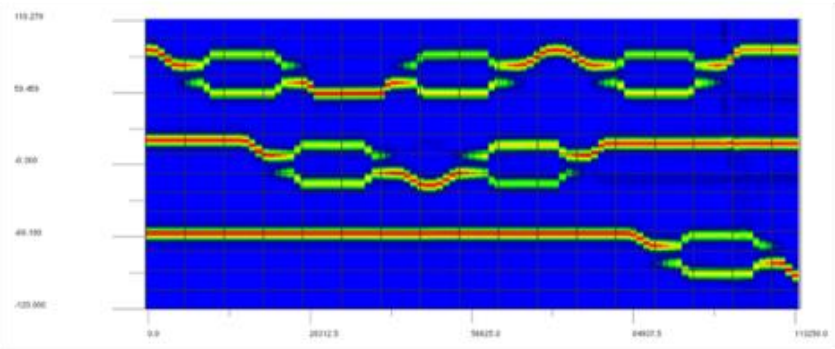

G2=0 G1=06.75 G0=0

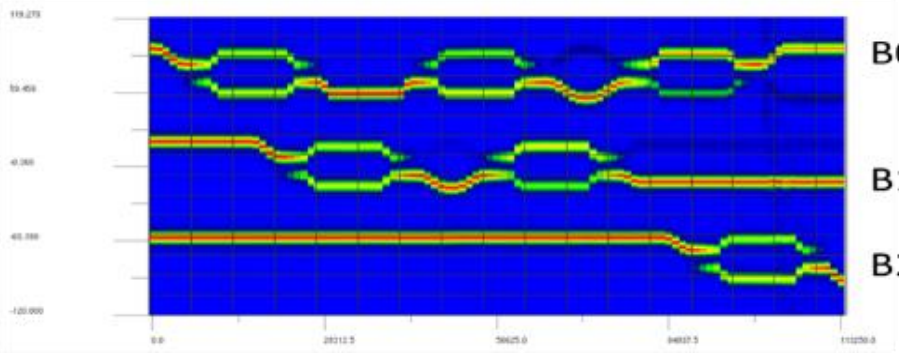

G2=0 G1=6.75 G0=6.75

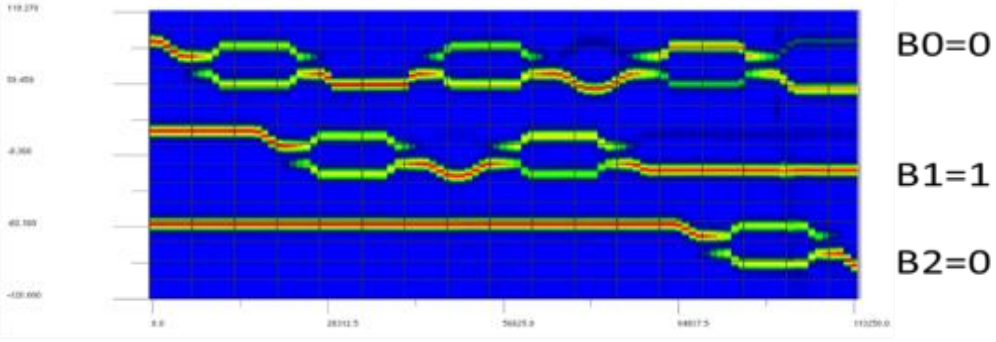

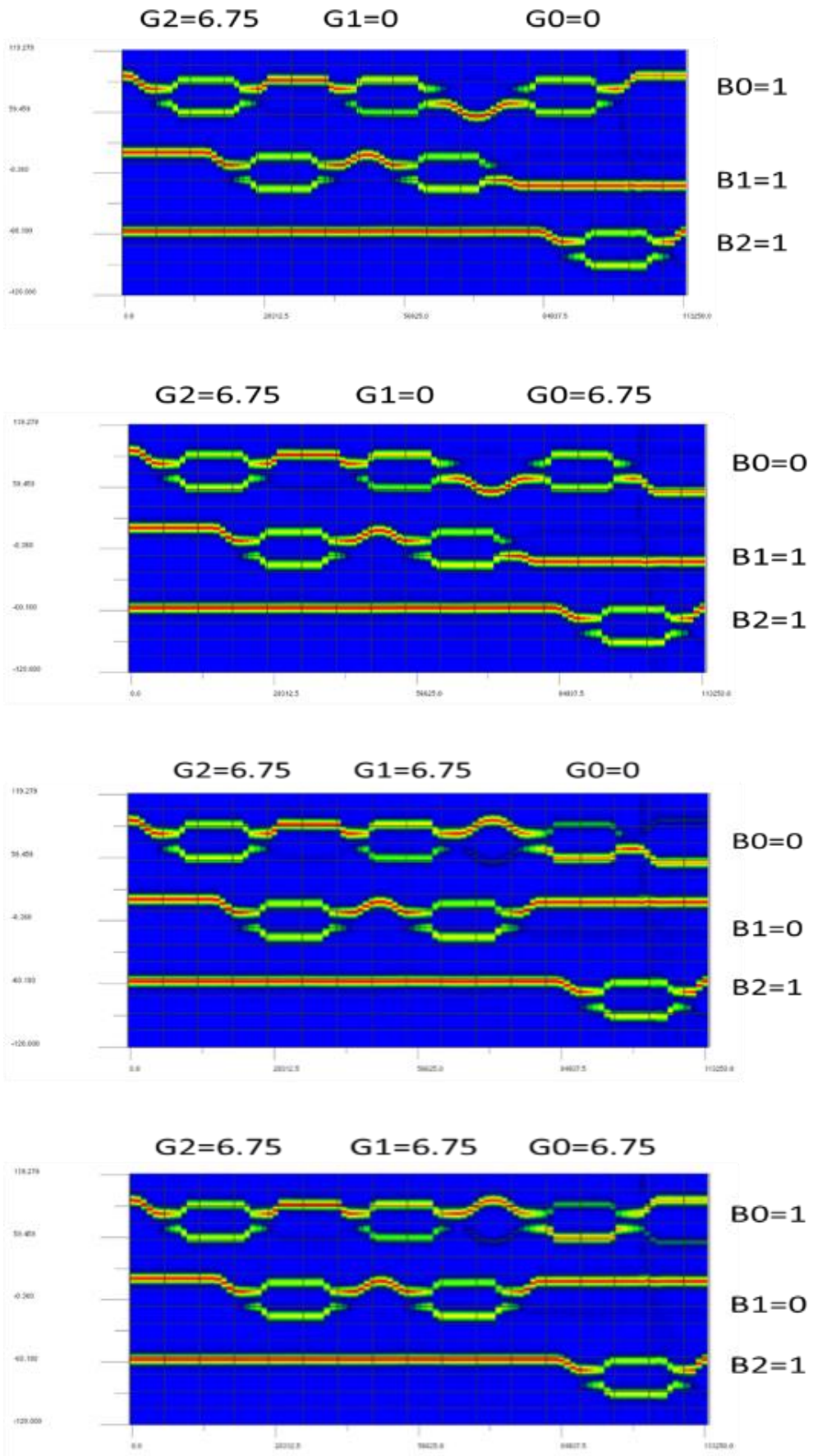

Fig. 4.4 Simulation result waveforms for 3-bit code convertor.

The extinction ratio (ER) and insertion loss (IL) are the main figure of merit to determine that how good is the logical device. The high value of ER is favorable and represents that device is capable of distinguishing between the logical 1 and logical 0. The value of insertion loss should be as minimal as possible. The ER and IL are calculated using the following relations

$$ER = 10\,log_{10}\frac{P_{OH}}{P_{OL}} \tag{4.4}$$

$$IL = 10\,log_{10}\frac{P_{in}}{P_{out}} \tag{4.5}$$

Where

P_{out} is the output optical power,

P_{OH} is the output optical power corresponds to binary 1,

P_{OL} is the output optical power corresponds to binary 0,

P_{in} is the input optical power,

Input optical power is 1 dBm. The output power is measured at each output port in both cases i.e. binary 1 and binary 0. Table 4.2, depicts the calculated values for the extinction ratio and insertion loss of the proposed 3-bit code convertor logic.

Table 4.2

The extinction ratio and the insertion loss at output ports

Output port	Extinction Ratio (dB)	Insertion Loss (dB)
1	25.5	0.70
2	19.6	0.40
3	22.0	0.02
4	23.4	0.08
5	25.1	0.05
6	22.0	0.02

The extinction ratio is more than 20 dB at all ports except port 2 where it is 19.6 dB. So, overall we can say device is well capable of distinguishing the logical 1 & 0. The insertion loss is less than 0.1 dB for all output ports except port 1 & 2 and the reason is the optical path length is more for port 1 and port 2 outputs.

Hence, the 3-bit gray to binary code converter based on MZI structure can be used in the high speed and secure optical communication systems. The main bottleneck of this purposed device is the length of the device which can be reduced further by proper analysis and adding the MgO impurities across the S-band waveguide. The bending radius can be reduced without increasing the bending loss because the MgO doping improved the refractive index contrast.

Chapter 5

Reversible Logic based 2x1 Multiplexer

All optical reversible logic has been a primary area of research in the last decade. The reversible logic will play an important role in future computing technology i.e. Quantum Computing as it is a very power efficient technology [42]. Many designs have been proposed using different materials and different devices using reversible logic [43]. In this chapter, we propose an optimized 2×1 all optical reversible multiplexer using Ti-indiffused Lithium Niobate channel waveguiding structure. The proposed device offers high-speed conversion and acceptable losses. Information is not lost as the inputs are also available at the output in reversible logic.

5.1 Reversible logic

The reversible logic circuits in optical domain will play an important role in designing a power efficient optical devices. The reversible logic circuit can be defined as a device which has a unique mapping between its input vector and output vector [44]. In the other words, we can say that a reversible logic gate has an equal number of inputs and outputs. These devices have some special inputs and outputs along with the regular inputs and outputs, they defined below:

1. **Ancilla inputs:** The inputs which are constant either 1 or 0 in order to maintain the reversibility of the circuit is called as ancilla inputs or constant inputs.
2. **Garbage outputs:** The unused outputs are called as garbage outputs. Sometimes they are used to make reversible logic circuits.

The ancilla/constant inputs and garbage outputs should be as minimum as possible. The NOT gate is the simplest and basic reversible logic gate. The Fredkin and Toffoli are the 3x3 universal reversible logic gates. Some of the reversible logic gates are described in next section.

5.2 Revisable logic gates

All optical reversible gate is mainly designed using the semiconductor optical amplifier (SOA) based MZI switch because of its high switching speed and low power consumption. In the upcoming sub-sections we will define the basic working of SOA-MZI switch, Feynman and Toffoli logic gates.

5.2.1 SOA based MZI switch

The MZI structure can be used as EO-switch as described in previous chapters. The main difference in the regular MZI and SOA based MZI is that the interferometric arms are replaced with the semiconductor optical amplifiers [45]. The SOA will amplify the optical signal in optical domain itself. The logic block diagram of SOA-MZI is shown in figure 5.1 with the input signal as A and control signal as B. The output we are getting at bar port (o/p port-1) is AB and at cross port (o/p port-2) is AB'.

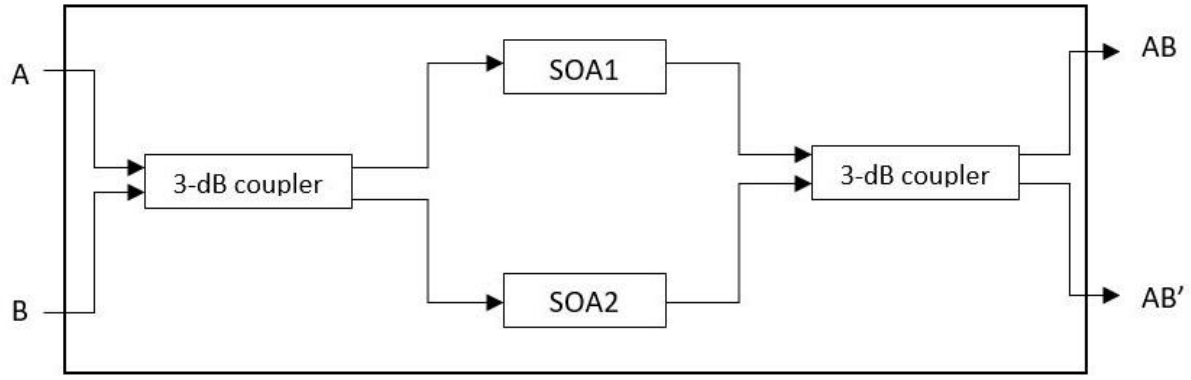

Fig. 5.1 The logical block diagram of 2x2 SOA-MZI switch.

The optical cost is defined as the number of SOA-MZI switch used in a particular all optical reversible logic circuit and the delta delay is defined as the delay taken by one SOA-MZI switch. Hence, for a single 2x2 SOA-MZI switch both optical cost and delay is unity.

5.2.2 Feynman gate

The Feynman gate is a 2x2 reversible logic gate and it is also called as controlled NOT gate (CNOT) [46]. The block diagram is shown in figure 5.2 (a) which consist of 2 inputs A & B and two outputs X & Y where X=A and Y= A XOR B. The implementation of

Feynman gate by using SOA-MZI switch is shown in figure 5.2 (b). It consists of two MZI switches, two beam-splitter (BS) and two beam-combiner (BC).

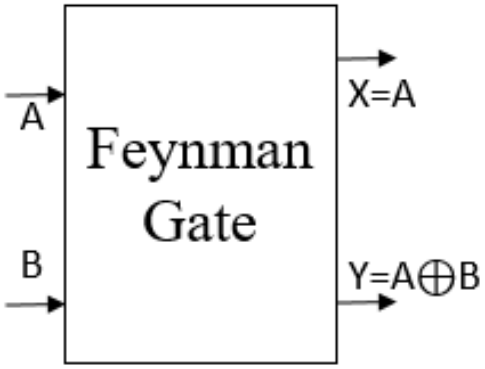

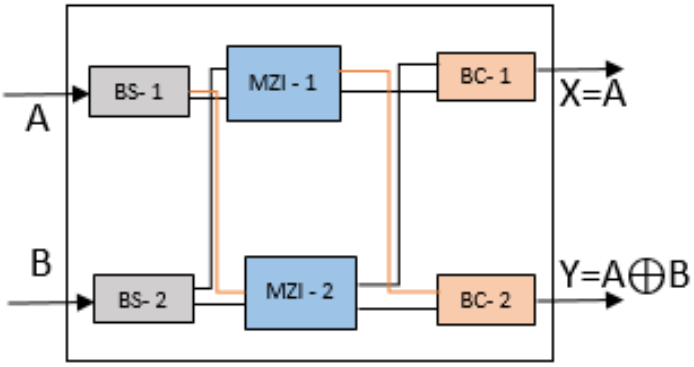

Fig. 5.2 (a) Block Diagram of Feynman Gate **Fig. 5.2 (b)** MZI based implementation.

The optical cost of Feynman gate is 2 as two MZI is used and delta delay is 1 unit as both MZI are operated in parallel. The beam-splitter and beam-combiner aren't contributed in optical cost.

5.2.3 Toffoli logic gate

The three input variant of the CNOT gate is called as Toffoli logic gate [47]. It is a 3x3 reversible logic gate i.e. it has 3 inputs (A, B & C) and 3 outputs (X, Y & Z) where, X=A, Y=B & Z=(A.B)⊕C. It has 3 garbage i.e. unused outputs also and the block diagram of the Toffoli logic gate is shown in figure 5.3.

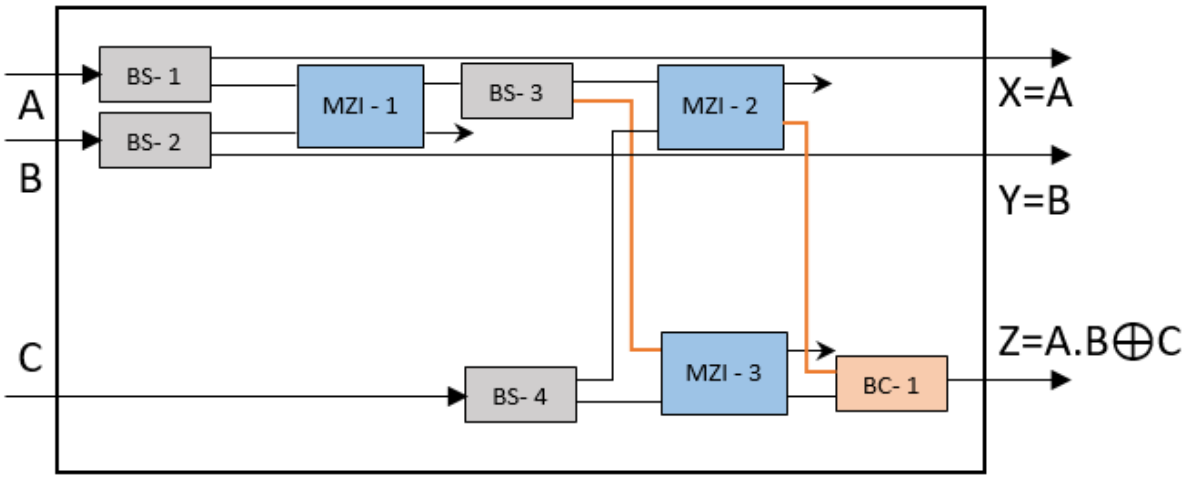

Fig. 5.3 Block diagram of Toffoli logic gate based on MZI structure.

The implantation of Toffoli logic gate based on MZI structure consist of three MZI switches, one beam-combiner and four beam-splitters. The optical cost is 3 and delta delay is 2 units. The Toffoli gate is a universal reversible gate like if C = 0, then Z = A.B i.e. AND gate or if C = 1, then Z = (A.B)' i.e. NAND gate. Other logic gates can also be derived using Toffoli gate.

5.3 2×1 MUX using Reversible Logic

The MUX is basically is a selector switch which selects one input among all inputs depending on the select lines and connects that the selected input to the output [48-50]. The basic 2×1 MUX has two inputs, one select line and one output; can be designed using the truth table given in table 5.1. The logical block diagram is given in figure 5.4, as it is designed on reversible logic so the number of inputs and outputs are equal. X and Y are the MUX inputs, S is a select line, Z is the MUX output and A is an additional input to make number of inputs and outputs equal and called as ancilla input, which is at logic 0. There are two garbage outputs also.

Table 5.1

Truth table for 2×1 MUX

Inputs			**Outputs**
X	**Y**	**S**	**Z**
0	0	0	0
0	0	1	0
0	1	0	0
0	1	1	1
1	0	0	1
1	0	1	0
1	1	0	1
1	1	1	1

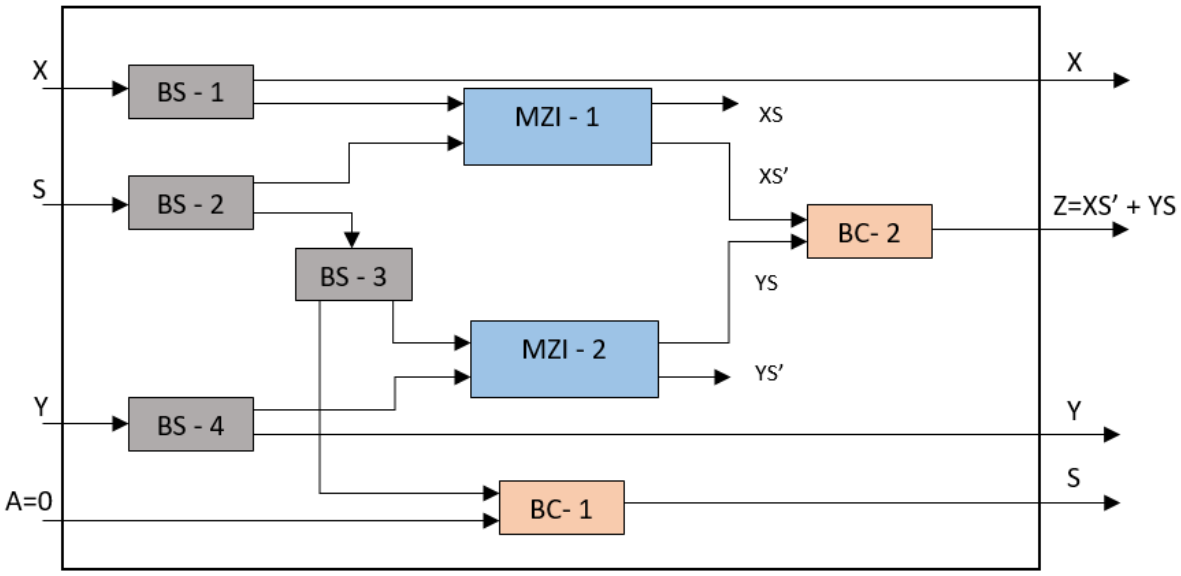

Fig. 5.4 The logical block diagram of 2×1 reversible MUX.

The purpose design of the 2x1 MUX has the 4x4 reversible configuration i.e. it has 4 inputs and 4 outputs. So, depending on the select line input S the output of the MUX i.e. Z can be equal to X (S=0) or Y (S=1). The optical cost of the 2x1 MUX is 2 as it is using 2 MZI switches, but they operate in parallel so the delta delay is one unit only.

Multiplexer is an important combinational circuit and it is also called as a universal circuit as all the logic gates can be designed by using the multiplexer circuit. As it is a basic circuit element for many combinational PICs, the power consumed by MUX should be optimized. In the dissertation work, we designed an optimized 2x1 MUX using the reversible logic based on SOA-MZI switch.

5.4 Implementation of Multiplexer

The 2×1 reversible MUX is implemented and simulated by using design tool: Optisystem. The SOA-MZI is designed using Ti-indiffused LN waveguide in OptiBPM and by using its scattering parameters it is exported into Optisystem to simulate the complete PIC of the 2x1 MUX. The layout of design is shown in figure 5.5, which consists of 2 MZI switches, 4 beam splitters and 2 beam combiners with 4 input/output ports, 2 unused outputs of MZI and one ancilla input (A=0). The simulation SOI-MZI is done with the central wavelength of 1.55 um and the TE polarized light wave. The only active device in the PIC of the multiplier is the SOA-MZI switch so the main power is dissipated in the switch only.

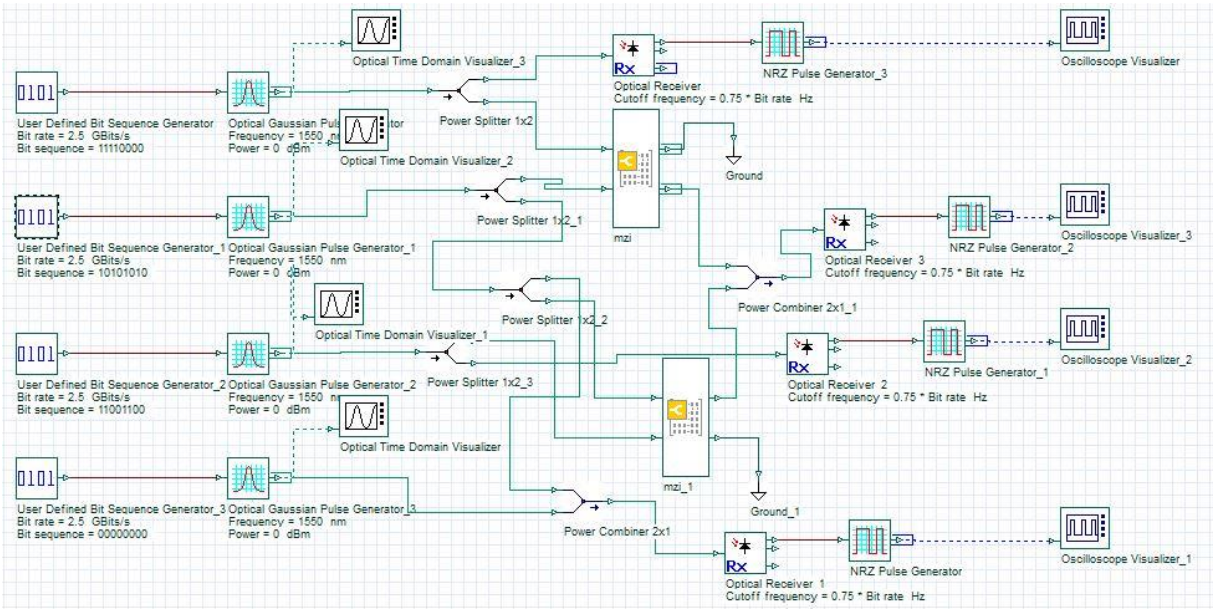

Fig. 5.5 The design layout of the purposed 2x1 MUX.

5.5 Simulation results and power optimization

The inputs are given to the MUX by using bits sequence generator followed by optical Gaussian pulse generator as X=11110000, S=10101010, Y=11001100 and A=0. The output we are getting as X=11110000, Z=11011000, Y=11001100 and S=10101010 which is detected by using an optical receiver and the waveforms are generated by using NRZ pulse generator. The waveforms of input signal are in optical domain and shown in figure 5.6 (a) and the outputs are in digital domain and shown in figure 5.6 (b).

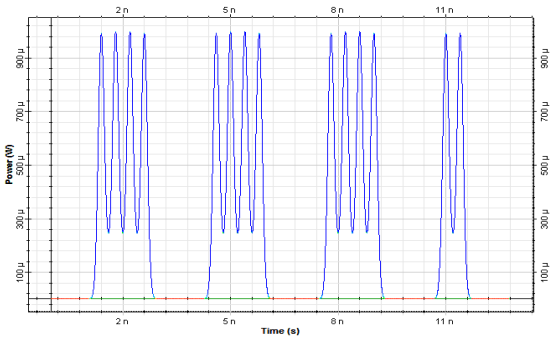

X=11110000

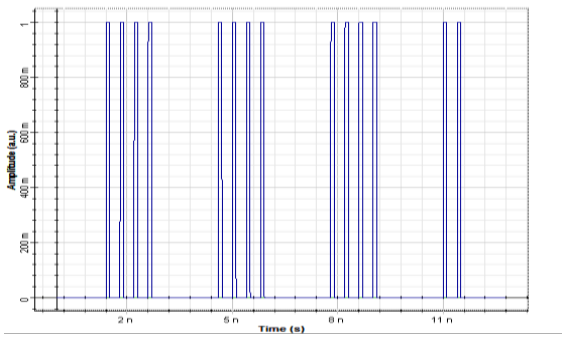

X=11110000

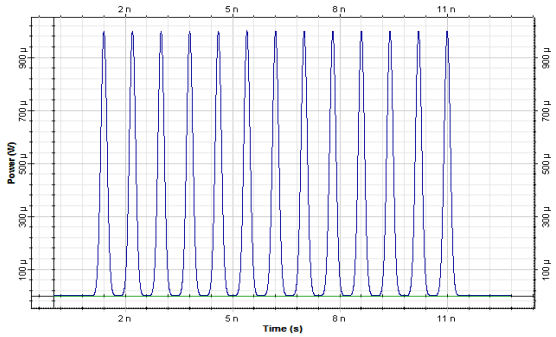

S=10101010

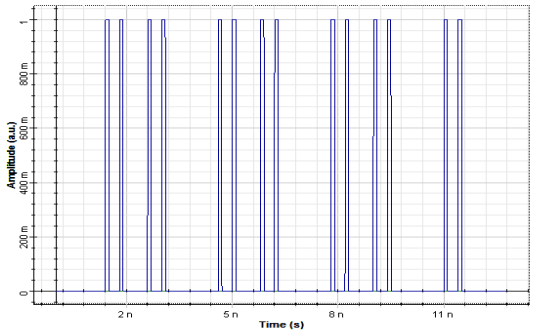

Z=11011000

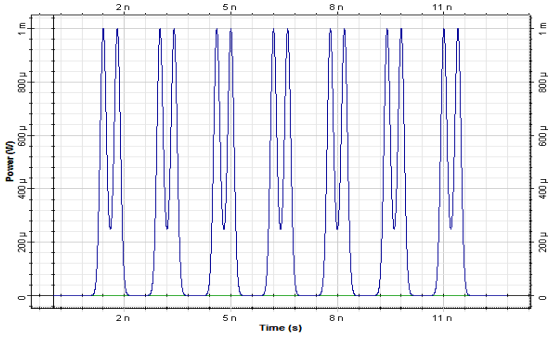

Y=11001100

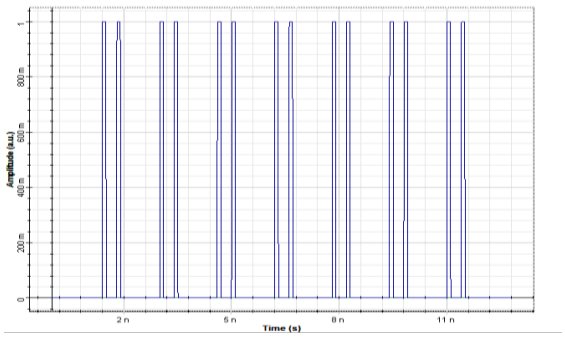

Y=11001100

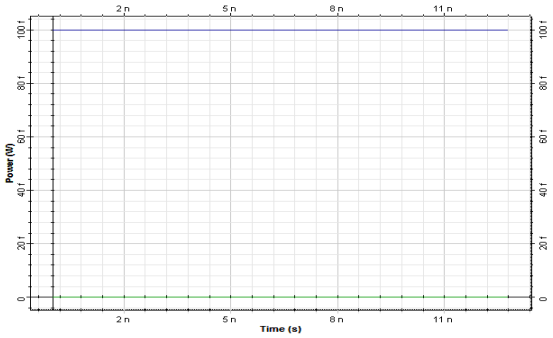

A=00000000

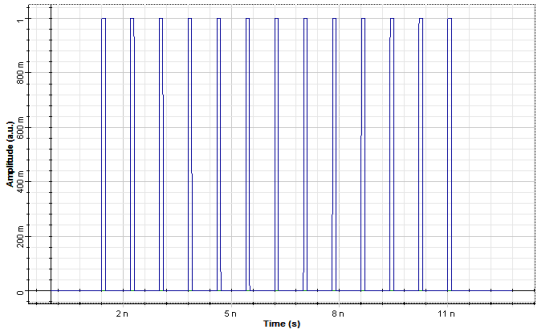

S=10101010

Fig. 5.6 Input and output waveforms of MUX.

The output power of the MZI switch can be optimized by varying interferometer arm length L and width of interferometer W. The variation of output power by varying L at different values of W is shown in figure 5.7 and the variation of power by varying W with keeping L constant is shown in figure 5.8.

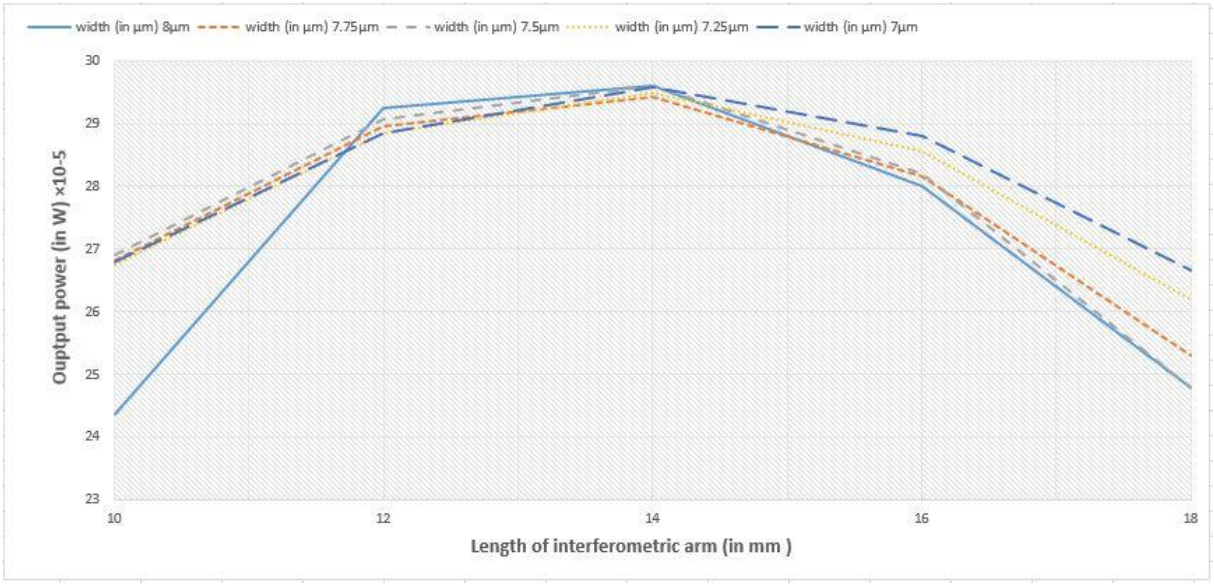

Fig. 5.7 The output power v/s L with W constant.

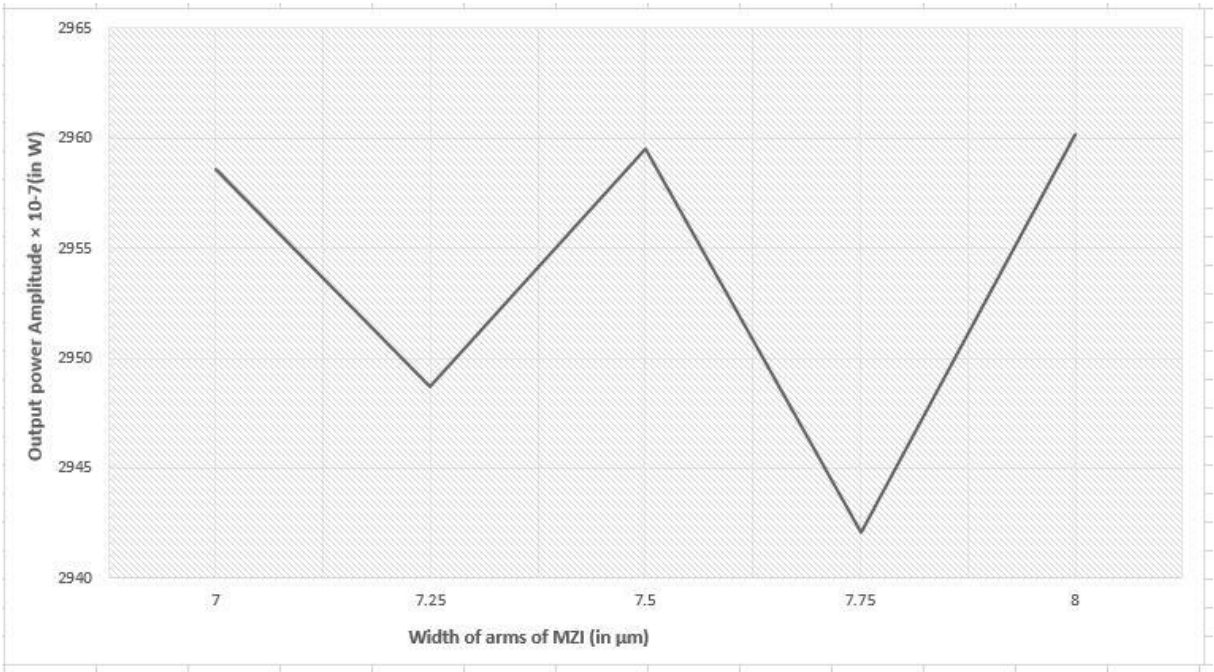

Fig. 5.8 The output power v/s W with L constant.

As seen in figure 5.7 the output power is maximum for interferometer length L=14000µm and from figure 5.8 the output is maximum for interferometer width W=8µm. So we can conclude that power consumption in MZI is optimized for interferometer length L=14000µm and width W=8µm. In future many other optimizations can be done to fabricate the PIC of reversible 2×1 MUX with least die size and least power consumption.

Chapter 6

Result Discussion and Conclusion

6.1 Result Discussion

In this dissertation work all optical photonics devices based on optical ring resonator and combinational circuits based on MZI structure using Lithium Niobate are proposed and numerically simulated. The principle of operation of ring resonator is based on Kerr effect and that of MZI is based on Electro-Optic effect. All the proposed logic devices have a high output power for high logic and also provide high extinction ratio. The Proposed notch filter based on LNOI resonates at 1.5709 um and notch bandwidth is 3.8 nm. The LNOI based OADM is designed for a 200 GHz channel spacing WDM system. The results are in the acceptable limits of the required system i.e. the FSR required is 3.2 THz and FWHM is 100 GHz. This OADM is optimized and cascaded to realize the eight channel multiplexer & demultiplexer for DWDM system with 100 GHz channel spacing. The insertion loss at the drop port is maximum 1.2 dB and the Q-factor is 1636. It can be used as Multiplexer as well as Demultiplexer in 8 channel DWDM systems. The data rate is 10 Gbps and hence this PIC can be used in DWDM-GPON network to enhance the performance.

Proposed 3-bit gray to binary code convertor based on MZI structure is analyzed for output power at each output port that can be used for high and low logic respectively. The extinction ratio at all output ports is calculated and the minimum obtained is 19.6 dB. The insertion loss is found to be 0.02 dB at port 3 & 6 and 0.7 dB at port 1.

For 2x1 MUX using SOA-MZI switch based on reversible logic, all the input combinations are verified. The SOA-MZI switch is only the active element of the PIC of the multiplexer. The power consumption of the PIC is optimized by optimizing the output power of the SOA-MZI switch. The power consumption in MZI is optimal with interferometric arm length L=14000 um and width of waveguide W= 8 um.

6.2 Conclusion

In this dissertation work all photonics devices and combinational circuits are proposed using the Lithium Niobate as substrate material. Lithium Niobate on insulator platform has been chosen as a material for the devices requiring high refractive index contrast. The structures are numerically simulated using finite difference time domain equations. All optical ring resonator based OADM devices are proposed and numerically simulated. In combinational circuits, 2x1 MUX and gray to binary code converters are designed. The proposed structures are all optical and do not require any O-E-O conversion. The proposed structure can be fabricated using LN-Photonics fabrication techniques and thus can become a fundamental component of an all optical signal processor in future.

Chapter 7

Future Scope

All optical photonics integrated circuits have been one of the most popular research area and in the last decade many devices using different platforms of PICs have been proposed. Numerous designs of all optical devices based on MZI structure, SOA-MZI switch, Photonic crystal and optical ring resonator have been reported and new designs are proposed. In this dissertation work, all optical logic devices based on LNOI microring resonator are proposed and numerically simulated. The channel waveguides are designed using Ti-indiffused LN. The main feature that set apart the logic gates reported in this work with all the designs proposed at 1550 nm wavelength and operated at high data rate i.e. at some Gigabits per second. Another major advantage is the high switch speed, high output power and low loss. Although the devices proposed in this dissertation work have some advantages over their predecessors but still there are some areas where LN-Photonic based PICs can be improved. These areas are listed below:

- The notch bandwidth and Q-factor which is sufficient for on chip signal processing but it has to be further improved if the designs need to be relevant in future.

- The cross-talk and other losses of OADM based multiplexer and demultiplexer for DWDM systems can be further reduced by applying the MgO doping along the ring resonator.

- The length of code converter is directly proportional to the number of bits of the code so for higher bit code convertor needs to be designed with advanced technology such that length of device will not grow very high.

References

[1] Agrawal, Govind P. Fiber-optic communication systems. Vol. 222. John Wiley & Sons, 2012.

[2] Papadimitriou, Georgios I., Chrisoula Papazoglou, and Andreas S. Pomportsis. "Optical switching: switch fabrics, techniques, and architectures." Journal of lightwave technology 21, no. 2 (2003): 384-405.

[3] Hunsperger, Robert G., and Jurgen R. Meyer-Arendt. "Integrated optics: theory and technology." Applied Optics 31 (1992): 298.

[4] Coldren, Larry A., Scott W. Corzine, and Milan L. Mashanovitch. Diode lasers and photonic integrated circuits. Vol. 218. John Wiley & Sons, 2012.

[5] Jalali, Bahram, and Sasan Fathpour. "Silicon photonics." Journal of lightwave technology 24, no. 12 (2006): 4600-4615.

[6] Poon, Joyce KS, Wesley D. Sacher, Ying Huang, and Guo-Qiang Lo. "Integrated photonic devices and circuits in multilayer silicon nitride-on-silicon platforms." In Optical Fiber Communications Conference and Exhibition (OFC), 2015, pp. 1-3. IEEE, 2015.

[7] Bogaerts, Wim, Martin Fiers, and Pieter Dumon. "Design challenges in silicon photonics." IEEE Journal of Selected Topics in Quantum Electronics 20, no. 4 (2014): 1-8.

[8] Rabiei, Payam, Jichi Ma, Saeed Khan, Jeff Chiles, and Sasan Fathpour. "Heterogeneous lithium niobate photonics on silicon substrates." Optics express 21, no. 21 (2013): 25573-25581.

[9] Marvin, J. Weber, and J. Weber. "Handbook of optical materials." Laser and Optical Science and Technology Series. The CRC Press. APPENDIX V. ISBN (2003): 978-0.

[10] Brinkmann, Ralf, Ingo Baumann, Manfred Dinand, Wolfgang Sohler, and Hubertus Suche. "Erbium-doped single-and double-pass Ti: $LiNbO_3$ waveguide amplifiers." IEEE journal of quantum electronics 30, no. 10 (1994): 2356-2360.

[11] Weis, R. S., and T. K. Gaylord. "Lithium niobate: summary of physical properties and crystal structure." Applied Physics A: Materials Science & Processing 37, no. 4 (1985): 191-203.

[12] Wooten, Ed L., Karl M. Kissa, Alfredo Yi-Yan, Edmond J. Murphy, Donald A. Lafaw, Peter F. Hallemeier, David Maack et al. "A review of lithium niobate modulators for fiber-optic communications systems." IEEE Journal of selected topics in Quantum Electronics 6, no. 1 (2000): 69-82.

[13] Singh, G., V. Janyani, and R. P. Yadav. "Modeling of a 2× 2 electro-optic Mach-Zehnder Interferometer optical switch with s-bend arms." Photonics Letters of Poland 3, no. 3 (2011): 119-121.

[14] Singh, Ghanshyam, Vijay Janyani, and R. P. Yadav. "Modeling of a high performance Mach--Zehnder interferometer all optical switch." Optica Applicata 42, no. 3 (2012).

[15] Kumar, Ajay, Santosh Kumar, and Sanjeev Kumar Raghuwanshi. "Implementation of full-adder and full-subtractor based on electro-optic effect in Mach–Zehnder interferometers." Optics Communications 324 (2014): 93-107.

[16] Gayen, Dilip Kumar, Tanay Chattopadhyay, Mantu Kumar Das, Jitendra Nath Roy, and Rajat Kumar Pal. "All-optical binary to Gray code and Gray to binary code conversion scheme with the help of semiconductor optical amplifier-assisted Sagnac switch." IET circuits, devices & systems 5, no. 2 (2011): 123-131.

[17] Hu, Zhefeng, Min Hou, Haiyang Liu, and Fushen Chen. "Investigation of All-Optical Tunable Notch Filter Based on Sum-Frequency Generation in a PPLN Waveguide." IEEE Photonics Journal 7, no. 6 (2015): 1-7.

[18] Kaalund, Christopher J. "Critically coupled ring resonators for add-drop filtering." Optics communications 237, no. 4 (2004): 357-362.

[19] Kim, Joo-Youp, Jeung-Mo Kang, Tae-Young Kim, and Sang-Kook Han. "All-optical multiple logic gates with XOR, NOR, OR, and NAND functions using parallel SOA-MZI structures: theory and experiment." Journal of Lightwave Technology 24, no. 9 (2006): 3392.

[20] Poberaj, Gorazd, Hui Hu, Wolfgang Sohler, and Peter Guenter. "Lithium niobate on insulator (LNOI) for micro-photonic devices." Laser & photonics reviews 6, no. 4 (2012): 488-503.

[21] Siewa, Shawn Y., Eric JH Cheunga, Mankei Tsanga, and Aaron J. Danner. "Integrated nonlinear optics: lithium niobate-on-insulator waveguides and resonators." In Proc. of SPIE Vol, vol. 10106, pp. 101060B-1. 2017.

[22] Saha, Soham, Siew Shawn Yohanes, Deng Jun, Aaron Danner, and Mankei Tsang. "Fabrication and characterization of optical devices on lithium niobate on insulator chips." Procedia Engineering 140 (2016): 183-186.

[23] Dai, Daoxin, Di Liang, and Liu Liu. "Introduction for the integrated photonics: challenges and perspectives feature." Photonics Research 3, no. 5 (2015): IP1-IP2.

[24] Volk, T., N. Rubinina, and M. Wöhlecke. "Optical-damage-resistant impurities in lithium niobate." JOSA B 11, no. 9 (1994): 1681-1687.

[25] Birnie, D. P. "Analysis of diffusion in lithium niobate." Journal of materials science 28, no. 2 (1993): 302-315.

[26] Holmes, R. J., and D. M. Smyth. "Titanium diffusion into LiNbO3 as a function of stoichiometry." Journal of applied physics 55, no. 10 (1984): 3531-3535.

[27] Nikolopoulos, John, and Gar L. Yip. "Accurate Modeling of the Index profile in annealed proton-exchanged LiNbO3 waveguides." In Integrated Optical Circuits, vol. 1583, pp. 71-82. 1991.

[28] Nikolopoulos, John, and Gar Lam Yip. "Theoretical modeling and characterization of annealed proton-exchanged planar waveguides in z-cut $LiNbO_3$." Journal of lightwave technology 9, no. 7 (1991): 864-870.

[29] Choubey, R. K., P. Sen, P. K. Sen, R. Bhatt, S. Kar, V. Shukla, and K. S. Bartwal. "Optical properties of MgO doped LiNbO 3 single crystals." Optical Materials 28, no. 5 (2006): 467-472.

[30] Sakashita, Yukio, and Hideo Segawa. "Preparation and characterization of $LiNbO_3$ thin films produced by chemical-vapor deposition." Journal of applied physics 77, no. 11 (1995): 5995-5999.

[31] Lansiaux, X., E. Dogheche, D. Remiens, M. Guilloux-Viry, A. Perrin, and P. Ruterana. "$LiNbO_3$ thick films grown on sapphire by using a multistep sputtering process." Journal of Applied Physics 90, no. 10 (2001): 5274-5277.

[32] Gitmans, F., Z. Sitar, and P. Günter. "Growth of tantalum oxide and lithium tantalate thin films by molecular beam epitaxy." Vacuum 46, no. 8 (1995): 939-942.

[33] Bogaerts, Wim, Peter De Heyn, Thomas Van Vaerenbergh, Katrien De Vos, Shankar Kumar Selvaraja, Tom Claes, Pieter Dumon, Peter Bienstman, Dries Van

Thourhout, and Roel Baets. "Silicon microring resonators." Laser & Photonics Reviews 6, no. 1 (2012): 47-73.

[34] Little, Brent E., Sai T. Chu, Hermann A. Haus, J. Foresi, and J-P. Laine. "Microring resonator channel dropping filters." Journal of lightwave technology 15, no. 6 (1997): 998-1005.

[35] Godbole, Abhishek, Prathmesh Pravin Dali, Vijay Janyani, Takasumi Tanabe, and Ghanshyam Singh. "All Optical Scalable Logic Gates Using Si_3N_4 Microring Resonators." IEEE Journal of Selected Topics in Quantum Electronics 22, no. 6 (2016): 326-333.

[36] Godbole, Abhishek, Prathmesh P. Dali, G. Singh, and Takasumi Tanabe. "Microring resonator based all optical XOR and XNOR logic gates." In Computational Techniques in Information and Communication Technologies (ICCTICT), 2016 International Conference on, pp. 540-543. IEEE, 2016.

[37] Wang, Tzyy-Jiann, Chia-Hong Chu, and Che-Yung Lin. "Electro-optically tunable microring resonators on lithium niobate." Optics letters 32, no. 19 (2007): 2777-2779.

[38] Wu, Danning, Yuanda Wu, Yue Wang, Junming An, and Xiongwei Hu. "Four-channel optical add-drop multiplexer based on dual racetrack micro-ring resonators." Optics Communications 354 (2015): 386-391.

[39] Papaioannou, S., G. Dabos, K. Vyrsokinos, G. Giannoulis, A. Prinzen, C. Porschatis, M. Waldow, D. Apostolopoulos, H. Avramopoulos, and N. Pleros. "Eight-channel second-order ring resonator based SOI multiplexers/demultiplexers for optical interconnects." In Optical Communication (ECOC), 2014 European Conference on, pp. 1-3. IEEE, 2014.

[40] Kumar, Ajay, Santosh Kumar, and Sanjeev Kumar Raghuwanshi. "Implementation of XOR/XNOR and AND logic gates by using Mach–Zehnder interferometers." Optik-International Journal for Light and Electron Optics 125, no. 19 (2014): 5764-5767.

[41] Mehra, Rekha, Shikha Jaiswal, and Hemant Kumar Dixit. "Ultrafast all-optical 4-bit digital encoders using differential phase modulation in semiconductor optical amplifier-Mach-Zehnder interferometer configuration." Optical Engineering 52, no. 3 (2013): 035202-035202.

[42] Shende, Vivek V., Aditya K. Prasad, Igor L. Markov, and John P. Hayes. "Reversible logic circuit synthesis." In Proceedings of the 2002 IEEE/ACM international conference on Computer-aided design, pp. 353-360. ACM, 2002.

[43] Kotiyal, Saurabh, Himanshu Thapliyal, and Nagarajan Ranganathan. "Mach-Zehnder interferometer based all optical reversible nor gates." In VLSI (ISVLSI), 2012 IEEE Computer Society Annual Symposium on, pp. 207-212. IEEE, 2012.

[44] Mamataj, Shefali, Dibya Saha, and Nahida Banu. "A Review of Reversible Gates and its Application in Logic Design." American Journal of Engineering Research 3, no. 4 (2014): 151-161.

[45] Ju, H., S. Zhang, D. Lenstra, H. De Waardt, E. Tangdiongga, G. D. Khoe, and H. J. S. Dorren. "SOA-based all-optical switch with subpicosecond full recovery." Optics Express 13, no. 3 (2005): 942-947.

[46] Desoete, Bart, and Alexis De Vos. "Feynman's reversible logic gates, implemented in silicon." In Proceedings of the 6 th Advanced Training Course on Mixed Design of VLSI Circuits, Technical University Lodz, Napieralski A.(ed.), Krakow, juni 1999, pp. 497-502. 1999.

[47] Arun, Vanya, Ashutosh Kr Singh, N. K. Shukla, and D. K. Tripathi. "Design and performance analysis of SOA–MZI based reversible toffoli and irreversible AND logic gates in a single photonic circuit." Optical and quantum electronics 48, no. 9 (2016): 445.

[48] Kumar, Santosh, and Chanderkanta Chauhan. "Design of reversible multiplexer using electro-optic effect inside lithium niobate-based Mach–Zehnder interferometers." Optical Engineering 55, no. 11 (2016): 115101-115101.

[49] Katti, Rohan, and Shanthi Prince. "Implementation of a reversible all optical multiplexer using Mach-Zehnder interferometer." In Signal Processing,

Informatics, Communication and Energy Systems (SPICES), 2015 IEEE International Conference on, pp. 1-4. IEEE, 2015.

[50] Datta, Kamalika, and Indranil Sengupta. "All optical reversible multiplexer design using Mach-Zehnder interferometer." In VLSI Design and 2014 13th International Conference on Embedded Systems, 2014 27th International Conference on, pp. 539-544. IEEE, 2014.

List of Publications

Journal Publications

1. Harsh Kumar, Vijay Janyani, Buryy Oleh, Ubizskii Serhij, Sugak Dmytro, and Ghanshyam Singh. "Eight channel Optical Add Drop Multiplexer based on Ring Resonator using LNOI channel waveguides" Journal - Acta Physica Polonica A (communicated).

Conference Proceedings

1. Harsh Kumar, Vijay Janyani, Buryy Oleh, and Ghanshyam Singh. "Study of Optical Properties of Magnesium Doped Lithium Niobate: A Review", IETE Zonal Seminar North, March, 2016.
2. Harsh Kumar, Vijay Janyani, Buryy Oleh, and Ghanshyam Singh. " A review of surface geometric techniques suitable for Lithium Niobate based all optical devices" Proc. of OSA Young Student Congress on Photonic Technologies, OSA_YSC_107, PP. 18-21, April, 2016.
3. Harsh Kumar, Vijay Janyani, Buryy Oleh, Ubizskii Serhij, Sugak Dmytro, and Ghanshyam Singh. "Optical Ring Resonator Based Notch Filter Using Lithium Niobate on Insulator (LNOI)." COMSOL Conference 2016, Bangalore on October, 2016.
4. Harsh Kumar, Vijay Janyani, Buryy Oleh, Ubizskii Serhij, Sugak Dmytro, and Ghanshyam Singh. "Ring Resonator based Optical Add Drop Multiplexer Using Lithium Niobate on Insulator Channel Waveguides." In International Conference on Fibre Optics and Photonics, pp. W3A-15. Optical Society of America, 2016.
5. Harsh Kumar, Laxman Kumar, Vijay Janyani, Buryy Oleh, Ubizskii Serhij, and Ghanshyam Singh. "Gray to Binary Code Converter Using Ti-indiffused Lithium Niobate Based Mach-Zehnder Interferometer." Springer sponsored International Conference on Opto-electronics and Applied Optics (Optronix-2016), Kolkata, August, 2016.

6. Harsh Kumar, Sanjeev Jain, Manish Tiwari, Buryy Oleh, Ubizskii Serhij, Vijay Janyani, and Ghanshyam Singh. "Optimized 2×1 Multiplexer based on Reversible Logic using Titanium indiffused Lithium Niobate channel waveguides." International Conference on Optical and Wireless Technologies, Springer, Jaipur, India, March, 2017.